P. Kotsovinos, E. Rackauskaite, E. Christensen, A. Glew, E. O'Loughlin, H. Mitchell, R. Amin, F. Robert, M. Heidari, D. Barber, G. Rein and J. Schulz (2022) Fire dynamics inside an open-plan compartment with an exposed CLT ceiling and glulam columns: *CodeRed #01*, Fire and Materials. https://doi.org/10.1002/FAM.3049

Fire dynamics inside a large and open-plan compartment with exposed timber ceiling and columns: *CodeRed #01*

P. Kotsovinos[1], E. Rackauskaite[1], E. Christensen[1], A. Glew[1], E. O'Loughlin[1], H. Mitchell[2], R. Amin[2], F. Robert[3], M. Heidari[3], D. Barber[4], G. Rein[2], J. Schulz[1]

[1] Fire Engineering, Arup, London, UK

[2] Department of Mechanical Engineering, Imperial College London, UK

[3] Fire Testing Centre, CERIB, France

[4] Fire Engineering, Arup, Melbourne, Australia

ABSTRACT

There is an increasing global demand to build from timber as it is a sustainable and attractive material. One of the key challenges associated with timber buildings is their performance in a fire, in particular for medium and high-rise buildings and when timber is exposed. Research on this topic to date has been performed in compartments smaller than 84 m^2 which does not capture the fire dynamics of large compartments. This paper presents the first in a series of experiments carried out inside a large purpose-built, open-plan compartment with a floor area of 352 m^2. The large-scale compartment had a fully exposed unloaded cross-laminated timber (CLT) ceiling and glued laminated timber (glulam) columns, made with adhesives that have been tested to noy exhibit char fall-off in fire. At 352 m^2 floor area, this is currently the largest compartment fire experiment carried out globally. The compartment characteristics and the arrangement of wood crib mimicked the previous series of experiments in Poland in a non-combustible compartment by Rackauskaite et al. (2021). The experiment was instrumented with thermocouples measuring the gas temperature in the compartment, , and above two of the openings, as well as the temperature within the timber members. Plate thermometers were also included to measure the heat flux to the ceiling and of the external flaming. Additionally fixed and drone mounted cameras captured the fire. A protected steel column was added to calculate the equivalent fire exposure when compared to a standard fire resistance furnace test. The experiment was allowed to burn out without firefighting intervention. Continuous measurements were taken for 48 h. The wood crib was ignited at one end of the compartment. Flames rapidly spread across the timber ceiling to the other end of the compartment with the rest of the wood crib being involved in the fire at 5 min 36 s from ignition. The total duration of the fire was 22 min 30 s, at which time visible flaming ceased. Significant external flaming was observed through the openings in the order of 3 m in height but varied with position as the fire travelled across the compartment. Analysis of the experimental results and camera footage showed that the presence of the timber structure approximately doubled the heat release rate compared to the value expected from the wood crib alone. Smouldering combustion of the timber members continued for hours after the cessation of flaming, burning in several hotspots, resulting in holes through the CLT slab. This paper improves the understanding of fire dynamics for open-plan exposed timber compartments and has shown that issues such as external flaming, smouldering and the increase in heat release rate need to be considered when deriving practical design solutions.

1 INTRODUCTION

In the pursuit of the net-zero agenda set by the global community to fight climate change, more architects and engineers have turned their attention to heavy/mass timber as an alternative structural material to concrete and steel which are the materials predominantly used in building construction. Mass timber can be a more sustainable material, so could help in delivering these societal goals and numerous timber buildings are already being built globally. However, several stakeholders (engineers, approval authorities, fire authorities, testing laboratories, insurers, etc.) have also raised concerns with regards to the use of mass timber for medium and high-rise buildings where fire safety and the avoidance of structural collapse in the event of a fully developed fire is paramount. Structural timber is a combustible material and therefore when left exposed (i.e. not encapsulated), compartment fire dynamics will be altered due to the additional fuel load coming from the burning and charring of the timber [1]. Understanding fire dynamics in large timber compartments is one of the important knowledge gaps that exist which needed to be filled to establish credible design fire scenarios and to inform fire safety design methods for timber buildings that adequately mitigate risks introduced by the timber construction.

There is a limited number of compartment fire experiments with exposed timber construction. The experiments with contemporary timber (engineered) materials and dense instrumentation at the time of publication are reviewed here. Hadden et al. [2] and Bartlett et al. [3] present a series of compartment fire experiments (7.4 m^2 in floor area, A) to evaluate the impact of combustible CLT linings on compartment fire behaviour by varying the number of exposed surfaces. Emberley et al. [4] also present compartment fire experiments (A = 12.25 m^2) of a similar nature where the number of exposed CLT surfaces are varied to investigate impact on fire dynamics. Su et al. [5] carried out a number of compartment fire experiments (A = 41.86 m^2) at NIST with the intent to understand the impact of exposed timber on the contribution to the fire development and the effect of gypsum board protection over the timber on delaying or preventing involvement of the CLT in the fire under varied ventilation conditions. McNamee et al. [6] presented the findings of the "Epernon Fire Test Programme", an experimental campaign aimed at studying and comparing the fire dynamics and structural response of compartments (A = 24 m^2) with loaded CLT and concrete ceilings under a range of ventilation regimes leading to both fuel and ventilation controlled fires; the exposed CLT slab in one experiment was found to have collapsed the morning after the compartment fire experiment. More recently, Brandon et al. [7] published the findings of five compartment fire tests carried out by RISE, involving CLT slabs and glulam beams and columns. The compartments had surface areas of exposed mass timber equal to and up to two times the area of the floor plan (A = 47.95 m^2). The largest compartment fire experiments to date with exposed CLT (A = 83.54 m^2 per floor) have been carried out by Zelinka et al. [8] in a two-storey mass timber building. A series of 5 experiments were carried out in an apartment style structure varying the amount of exposed timber structure, and presence and activation of sprinklers.

Key fire dynamics observations relating to all of the aforementioned compartment fire experiments [2]–[8] with exposed timber carried out to date are:

- Heat release rates (HRR) are greater in compartments with exposed timber surfaces due to the additional fuel from the timber.
- In some experiments fire growth was found to be faster in combustible compartments and flashover (as defined by Drysdale [9]) was reached sooner.
- Longer fire durations are observed in combustible compartments, particularly where ventilation is limited.
- Compartments with combustible surfaces experience greater external flaming as there is insufficient oxygen available inside the compartment to combust all available pyrolysis gases, resulting in significantly higher radiation on nearby buildings.
- Whether the flaming combustion of the timber finishes when the flaming of the fuel finishes depends on the arrangement of the exposed surfaces, number and area of exposed timber surfaces as well as other factors that are not possible to control by design, such as weather conditions.
- Those types of CLT that are susceptible to char fall-off (i.e. losing part of the charred layer exposing fresh timber in the fire) may experience increased charring and lead to the fire reaching a "secondary flashover" or not reaching a decay phase after the contents have burnt due to fuel being continuously added to the fire from the structure itself.

Having reviewed the aforementioned experiments, Rackauskaite et al [10] note that the largest mass timber compartment tested to date is only 84 m^2 in floor area which is more representative of rooms in residential and hotel uses. As a result, these experiments are not necessarily representative of larger compartments such as open-plan offices and retail with proposed floor areas in the range 1,000 - 4,600 m^2, commonly used in the design of commercial buildings. The authors called for further research to be undertaken to confirm whether findings from smaller compartments (< 100 m^2 in floor area) apply to large compartments with exposed timber too. Existing compartment fire experiments and modern design aspirations are shown in Figure 1 [11].

It is critical to understand the effects of the exposed mass timber on fire dynamics of open-plan compartments in order to safely allow the use of exposed timber in fire safety design. For non-combustible compartments, fire dynamics can differ significantly between small compartments and large open-plan compartments. In large, open-plan non-combustible compartments, travelling fires have been observed. These are fires which burn over a localised area and spread along the compartment [12], [13]. In addition, in large compartments fires tend to be fuel controlled rather than ventilation controlled as is often the case for small compartments [14], [15] . No experimental evidence currently exists to investigate the fire dynamics experienced in large compartments (> 100 m^2) with exposed timber and how these differ from small compartments and non-combustible large compartments.

Richter et al. [16] has assessed the thermal response (charring rate and zero strength layer) of timber slabs under a range of design fires (travelling fires, Eurocode parametric fires, and the standard fire). The authors adopted design fire models used typically for non-combustible compartments and, similarly to Rackauskaite et al [10], highlighted the lack of validated design fire tools for open-plan compartments with exposed timber.

This paper presents *CodeRed #01* – the first fire experiment in a series carried out inside a purpose-built, open-plan compartment with a floor area of 352 m^2. Note the term *CodeRed* experiments has been established to group all the experiments together for future searchability. The large-scale compartment had a fully exposed CLT ceiling and glued laminated timber ("glulam") columns. At 352 m^2 floor area, this is the largest compartment fire experiment with exposed timber carried out to date as illustrated in Figure 1. This paper therefore aims to fill some of the gaps in understanding compartment fire dynamics in open-plan compartments with exposed timber by presenting experimental data that can then be used by researchers in the future to develop theoretical models for large compartments.

The compartment is based on a non-combustible building previously used for travelling fire experiments and therefore allows for a future comparison of fire dynamics in combustible and non-combustible compartments [11], a detailed comparison is outside the scope of this paper.

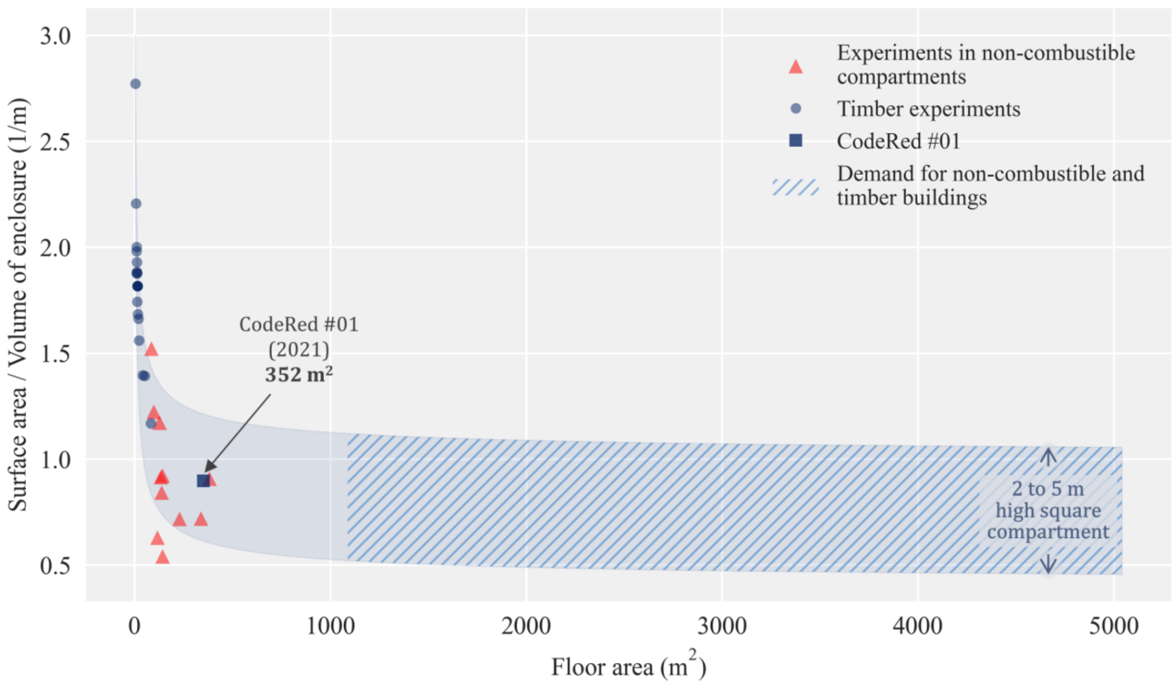

Figure 1. Comparison of the surface area to volume ratio of compartments within which experiments have been carried out to date, and demand for non-combustible and timber buildings worldwide. Shaded area represents a range of typical surface area to volume of enclosure ratios for a rectangular compartment with floor to ceiling heights between 2 m and 5 m.

2 *CodeRed #01*

2.1 The facility

A new facility was built at CERIB's site in Epernon, France that enables variation in both fuel load, ventilation, and ceiling construction; parameters which are planned to be varied in future experiments. The parameters build on a series of experimental campaigns in 2017 and 2019, known as *x-ONE* [11] and *x-TWO* [17], that were conducted in a non-combustible structure in Poland with a floor area of ~380 m^2 to study travelling fire dynamics in open-plan compartments. These experiments are currently the largest compartment fire experiments to date in terms open-plan floor area [11], [17]. To compare the fire dynamics observed in these non-combustible compartments to those with exposed timber, a purpose built facility was designed to closely follow the characteristics of the existing building, 'Obora', in which the *x-ONE* and *x-TWO* campaigns were previously carried out.

Internally, the compartment is 10.27 m wide, 34.27 m long and 3.1 m high. The building was constructed from aerated concrete blocks (365 mm thick, 350 kg/m^3) to provide a robust non-combustible enclosure and support the hinge detail formed to support the ends of each CLT panel. A load bearing 34.27 m long concrete beam (0.25 m × 0.55 m) runs along the centreline of the compartment and is supported by 6 concrete columns (0.25 × 0.25 m) spaced 5.79 m to 6.80 m apart to support the centre of the CLT panels. The protection of the supporting structural elements is discussed in Section 2.3.

CodeRed #01 was built with a fully exposed CLT ceiling, two glulam columns and a protected steel column to evaluate their performance during and after a fire. The two glulam columns were installed 1.75 m offset from the centreline to the south west, at 16.64 and 31.60 m from the start of the compartment (12.22 and 27.18 m from ignition) for Column 1 and 2 respectively (see Figure 2). Further details of the CLT ceiling and glulam columns are provided in Section 2.2. The steel column was included to establish a comparative fire severity for a non-combustible structural member. The column section was HEB 200, was 3.05 m high and protected with two layers of 15 mm plasterboard to achieve a load-bearing fire resistance of 90 min. It was positioned between the two glulam columns, 24.21 m from the north west entrance (19.7 m from ignition location). None of the CLT ceiling, glulam or steel columns were load bearing as the experiment intent was to investigate compartment fire dynamics while minimising the risk of structural collapse to mitigate potential health and safety risks.

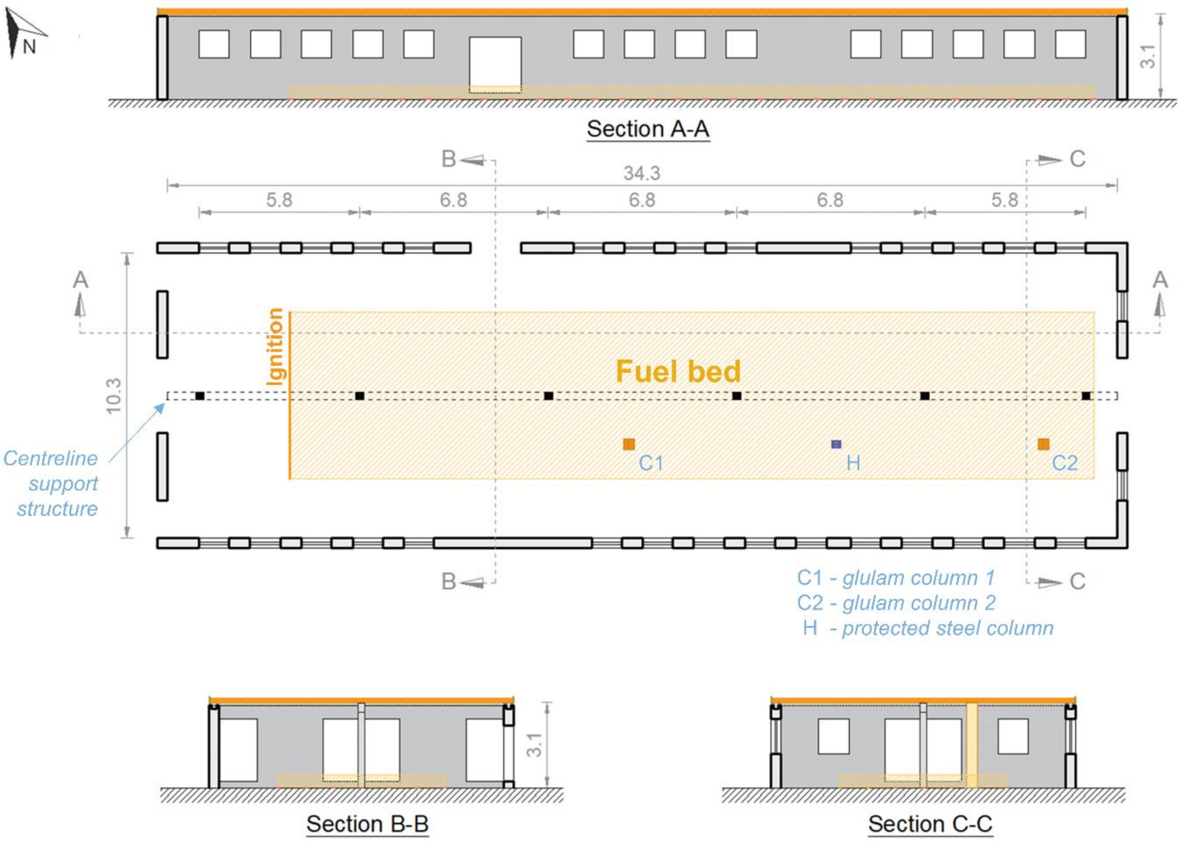

Figure 2. Floor plan and sections of the compartment used for the *CodeRed #01* experiment. Units in metres.

2.2 Timber ceiling and columns

The CLT ceiling comprises 5 ply (40-20-20-20-40 mm) spruce wood with MUF adhesive and was left without any protection throughout the compartment. The CLT ceiling was constructed of 14 panels laid side by side with each panel spanning the width of the compartment and centrally supported by the continuous concrete beam. 13 panels had dimensions of 2.50 m × 10.93 m, while the size of the edge panel at the south east entrance was 2.43 m × 10.93 m. Two intumescent seals were stapled in place between where two panels met and a surface mounted jointing board was installed on the top of the joint. The panels were fixed to the walls via a hinge support and rested on the centreline load bearing structure. The CLT was selected to achieve glue-line integrity (i.e. it does not show "char fall-off" behaviour) which was established via a 120 min standard fire test where the char line progressed through more than two adhesive layers and produced predictable and constant charring rates that were consistent with EN 1995-1-2. CLT that does not demonstrate "char fall-off" behaviour was chosen to avoid the known risk of char fall-off which can negatively impact fire dynamics and result in an undesirable feedback loop such as fire re-growth. That risk can be avoided by material selection, allowing focus on compartment fire dynamics while also reducing the number of variables that need to be considered.

The two glulam columns included in the experiment were 3.05m high with a cross-section of 0.4 m × 0.4 m. They were built from two 0.2 m × 0.4 m glulam members bonded together using a PUR adhesive to allow channels to be routed through the center of the columns for instrumentation (see Section 2.6 for more details) This enables the subsequent investigation of the interaction between CLT ceiling panels and exposed glulam columns, and to understand thermal penetration within timber columns. The instrumentation was fitted into the columns by the manufacturer, to the specification by CERIB.

The CLT and glulam was purchased directly from a large European supplier (non-aesthetic grade). A representative sample of the timber used in the CLT ceiling was measured, on the day of the experiment, to have a moisture content of 11.1 ± 0.2 % (on dry basis). The density of the CLT was 450 kg/m^3 (provided by the manufacturer), and an average heat of combustion of 18.79 MJ/kg for the CLT ceiling and the glulam columns was measured using bomb calorimetry.

2.3 Building protection

Key elements of the building structure were protected to prevent collapse, enable repeated use of the structure for future experiments, and protect instrumentation. The protection applied is presented in Figure 3.

The hinge connections to which the CLT ceiling panels connect were protected by filling the space around the connection with insulating wool as indicated in the middle and bottom right image of Figure 3. The centreline load-bearing structure was wrapped in insulating wool to protect the structure for future experiments (left image in Figure 3). Additionally, mineral wool was applied at the top and bottom of both the glulam and steel columns to prevent passage of flames at the top and to protect column instrumentation wires at the base (see Section 2.6). Columns did not extend to the ceiling as they were not loadbearing. Therefore, they were isolated from the fire at the top by the 50 mm thick mineral wool insulation compressed to 35 mm. The steel column was protected using two layers of plasterboards to give a 90 min fire protection in accordance with PV EFR-16-U-000563 (SINIAT) (top right image of Figure 3).

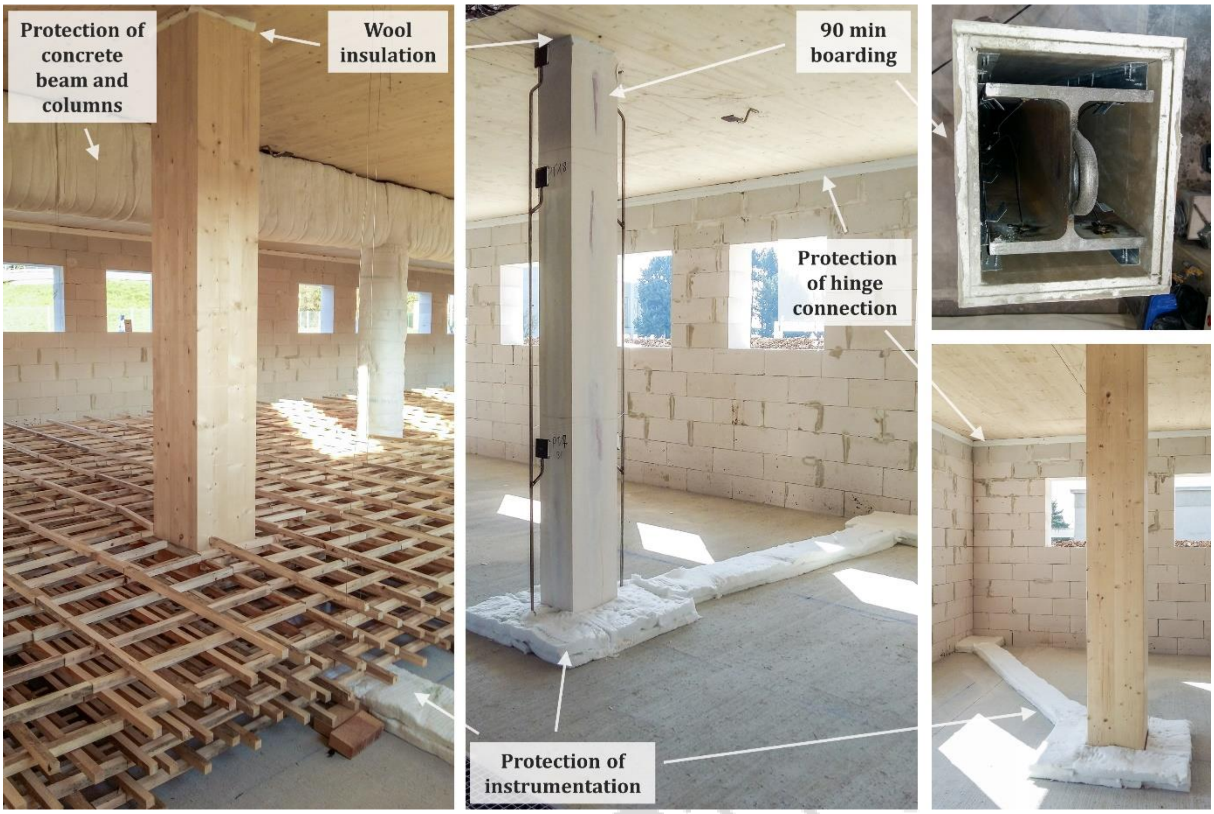

Figure 3. Protection of the key structural elements and instrumentation. The middle and bottom right images are taken before the construction of the wood crib.

2.4 Ventilation

The *CodeRed* building was constructed with 5 doors and 31 window openings (for opening dimensions see Table 1). It was intended for the ventilation to be nearly identical to the 'Obora' building used in *x-ONE* [11] and *x-TWO* [17], allowing for the direct comparison of results. All openings were left open to represent the conditions of an open-plan compartment with large ventilation and to minimise the likelihood of a ventilation-controlled fire.

In total, 20.5% of the compartment wall surface area constituted of openings (i.e. area of window opening, A_w = 57 m^2), resulting in an opening factor of 0.071 m$^{1/2}$ ($A_w\sqrt{h}/A_{total}$, where A_{total} is the total surface area including openings) with a weighted average opening height, *h*, of 1.49 m as defined in Annex A of Eurocode 1 [18]. Opening factors are commonly used to describe the amount of ventilation in a fire compartment. The higher the opening factor, the more likely the fire is to be fuel controlled.

Table 1. Opening dimensions along different elevations of the building used for the *CodeRed #01* experiment.

Building elevation	**Door openings** *(Number × Width × Height)*	**Window openings** *(Number × Width × Height)*
North west (*Sec A-A in Figure 2*)	1 × 2.76 m × 2.25 m 2 × 1.362 m × 2.25 m	*None*

Building elevation	Door openings *(Number × Width × Height)*	Window openings *(Number × Width × Height)*
North east (*Sec C-C in Figure 2*)	1 × 1.875 m × 2.00 m	14 × 1.09 m × 1.00 m
South east (*Sec B-B in Figure 2*)	1 × 2.76 m × 2.25 m	2 × 1.09 m × 1.25 m
South west	*None*	15 × 1.09 m × 1.00 m

2.5 Fuel bed

The fuel bed arrangement and density for *CodeRed #01* was based on that used for *x-ONE* [11] and *x-TWO.1* [17] experiments to enable comparisons. A continuous wood crib, covering a floor area of 174 m^2 (6 m × 29 m) was constructed 4.42 m from the north west entrance and was laid along the centre of the compartment finishing 0.85 m from the south east entrance.

The wood crib had an approximate fuel density of 374 MJ/m^2, equivalent to that originally used in the *x-ONE* and *x-TWO* experiments, and was chosen to limit the risk of significant damage to the structure but to still be within the range of typical fuel load densities in office buildings [13], [18].

The wood crib was arranged to have 11 stick layers with 4 sticks/m per each layer with additional layer at the bottom and at the top with 2 sticks/m (i.e. 13 stick layers in total). The wood crib was elevated from the ground by building it on top of bricks placed every 1 m to reduce heat losses to the concrete floor and enable air circulation below the crib. In the first meter of the crib, 5 mm thick wood fibreboard (cut into strips of 0.59 m × 0.2 m) was laid on the bottom 2 layers of sticks to facilitate the ignition of the crib as done for the *x-TWO* experiments [17]. Illustration of the fuel bed in shown in Figure 4.

For the wood crib, softwood sticks with the dimensions of 30 mm × 30 mm × 1000 mm, density of 392 - 526 kg/m^3 (average ~455 kg/m^3), heat of combustion of 19.05 MJ/kg, and moisture content of 13.5 ± 0.8 % (on dry basis) were used. The wood fibreboard had a density of 250 kg/m^3 and a heat of combustion of 19.016 MJ/kg. A random sample of 70 wood sticks was collected on the day of the experiment and weighed to obtain a representative average wood density. A sub-sample of 9 wood sticks were then oven dried at 105°C for four days to obtain their moisture content. Bomb calorimetry was used to measure the heat of combustion of the wood sticks and fibreboard. These values were used to determine the final fire load used in the experiment as detailed in the previous paragraph.

The ignition procedure for the fuel was the same as for both *x-ONE* and *x-TWO*. The fuel was ignited by placing a line of 12 pans (150 × 250 mm), each filled with 0.5 l methanol, below one end of the continuous wood crib (i.e. near the north west entrance) to study the natural flame spread across the compartment. The methanol was ignited simultaneously via a fuse to give a uniform line of ignition. The fire was ignited at 23:11:55 on March 9th, 2021. CERIB staff trained as fire fighters were present throughout the experiment as a preventative measure. However, no suppression was performed in *CodeRed #01*, allowing the fire to burn out naturally and enable the study of the fire dynamics including the long-term fire decay and smouldering behaviour of the CLT and the glulam columns. It should be noted that fire-fighters from the French fire brigade were also present in an observational role.

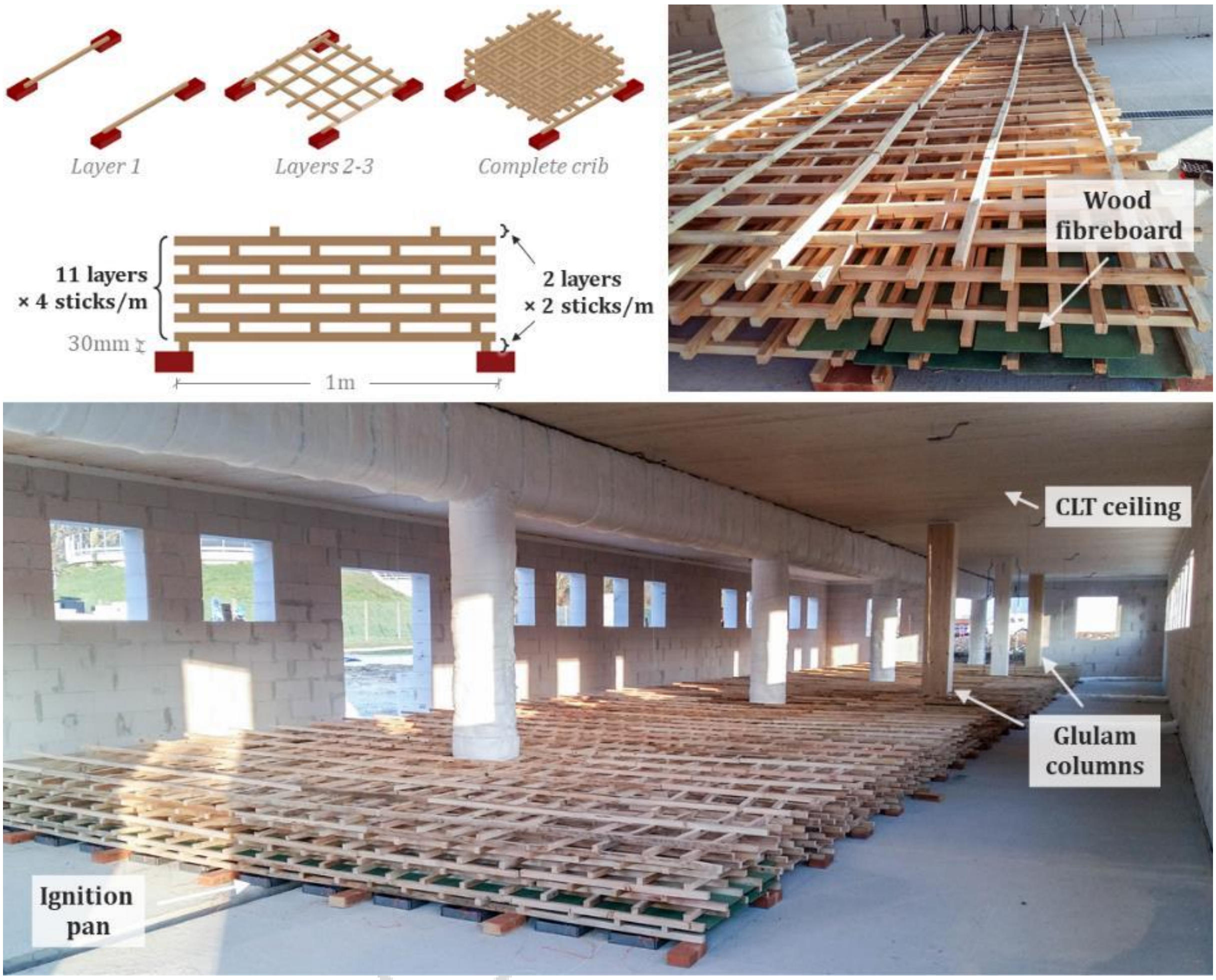

Figure 4. Illustration and photos of the final wood crib arrangement used as fuel for the *CodeRed #01* experiment. Wood stick dimensions were 30 mm × 30 mm × 1000 mm. Bottom image shows the completed wood crib.

2.6 Instrumentation

Extensive instrumentation was provided to measure the fire dynamics and the thermal exposure of the structure to the fire. The temperature development of the gas, CLT ceiling, glulam and steel columns were measured, as well as the incident heat flux received by the ceiling and protected steel column. Additionally, gas temperature and heat flux measurements were recorded of the external flaming from one door and one window. Finally, visual cameras were used to capture the internal fire spread dynamics, and external flaming behaviour. In total 200 type-K thermocouples, 28 plate thermometers, and 22 cameras were used as part of the experiment. The instrumentation layout is illustrated in Figure 5. The DAQ system used was Agilent 34 970 – 34 972.

Data was recorded for 60 hours to capture the temperature development within the timber elements during the cooling phase and any fire dynamics that occurred following the burn out of the crib, such as smouldering or transition to flaming. This behaviour is noted to be important with respect to structural capacity. To date, to the best of the knowledge of the authors, no such data exist which capture the timber behaviour for an extended duration following the experiment. As discussed in Section 1, an exposed CLT slab was found to have collapsed the morning after the compartment fire experiment in another experimental program, however no data was recorded to explain the mechanisms that resulted in the failure [6].

2.6.1 Gas temperatures

57 thermocouples (see Figure 5) were distributed across the compartment, organised into 17 thermocouple trees (T), to measure the gas temperature distribution and thermal exposure to the structure. The thermocouple placement was carefully selected to capture the vertical and horizontal temperature distribution while remaining consistent with the placement of thermocouples in *x-ONE* and *x-TWO* for direct comparison. As such, 9 thermocouples trees were placed near the centreline of the compartment: offset by 0.375 m to the south west from Gridline position B1-B9, and 4 were placed along the edge of the crib on both sides of the centreline: along Gridlines A and C at the intersection with gridlines 3, 5, 7, 9. The thermocouples were hung at 0.3, 1.0, 2.4, and 3.0 m above the floor level (FL) equating to 2.8, 2.1, 0.7 and 0.1 m below the ceiling level (CL). To optimise instrumentation and data processing, thermocouples at FL: +0.3 m (CL: -2.8 m) were only included in a limited number of locations (T12-T17).

To account for the radiative heat flux from the fire, the recorded thermocouple measurements were corrected using a methodology referred to as the β*-method,* first presented in *x-ONE* [11] and subsequently used in *x-TWO* [17]. The corrected gas temperature (T_g) was calculated as follows:

$$T_g = T_{TC} + \frac{\varepsilon\sigma}{h}(1-\beta)\cdot T_{TC}^4 \qquad (1)$$

Where the heat transfer coefficient, h, varies over the course of the experiment and is determined by evaluating the Nusselt number as in *x-ONE* and *x-TWO* [11], [17]. ε is the emissivity of the plate (assumed here to be 0.9 [11], [17]), T_{TC} is the recorded thermocouple temperature, σ is the Stefan Boltzmann constant and β is a non-dimensional correction factor.

As in *x-ONE* and *x-TWO*, the following correction factors were adopted: $1.17 \leq \beta \leq 1.25$. This range aims to capture the estimated uncertainty in radiative heating as well as the error associated with thermocouple measurements.

2.6.2 Incident heat flux

13 plate thermometers (PT) were installed horizontally, 0.1 m below and facing away from the ceiling (FL: +3.0 m) to be able to calculate the variation and development of incident heat flux

at the CLT ceiling. 8 plate thermometers were placed near the centreline: 5 of which were co-located with thermocouple trees (offset 0.375 m to the south west from Gridline B at the intersection with gridlines 1, 3, 5, 7, 9) and the remaining 3 (PT 11, PT 12, and PT13) were located such that they were consistent with *x-TWO*. 5 plate thermometers were installed along Gridline C and were also co-located with thermocouple trees. These were intended to capture the lateral variation in the incident heat flux.

2.6.3 Timber members' temperature profile

A total of 64 thermocouples were installed within the CLT ceiling (referred to as 'CLT' thermocouples) to measure the temperature development. They were placed at 5 evenly spaced locations along the compartment, aligning with gas temperature and plate thermometer measurements (vertical gridlines 2, 4, 6, 8, 10), and in two lateral positions: near the centreline (gridline B – 0.375 m) and along the edge of the crib (gridline C). Additional thermocouples were located within the CLT 0.1 m from the north east and north west face each of the glulam and steel columns. At all locations the CLT thermocouples were inserted from the back and placed at 20, 40, 60 and 80 mm from the internal exposed ceiling surface. Inserting thermocouples from the back is expected to introduce some error when compared to inserting thermocouples parallel to ceiling (i.e. inserted from the side)[19]. As the CLT performance is outside the scope of this paper, no further discussion is provided on correcting the measured values.

The two 400 × 400 mm glulam columns were instrumented to record temperatures using a total of 24 thermocouples. The columns were constructed by bonding two 200 × 400 mm glulam members together using a PUR adhesive with one internal glulam face routed with small channels to allow all thermocouple wires to be fed centrally though the column such that no thermocouple wires were exposed to the fire. The thermocouples were in groups of eight thermocouples located at three heights within each column: 0.3, 1.0, and 3.0 m above the floor level (CL: -2.8, -2.1, -0.1 m). For each grouping of thermocouples, four were located at the middle of the column width, at 20, 40, 60 and 80 mm from the exposed surface, facing north east ('Face A') and four were located on the opposite side, again located 20, 40, 60 and 80 mm from the exposed surface, with these staggered from the middle of the column, facing south west ('Face B'). The thermocouple tips were held in place through small pins.

2.6.4 Protected steel column

The protected steel column was instrumented to mimic the instrumentation of the standard fire test EN 13381-4. 15 thermocouples were mounted directly onto the surface of the column at 0.3, 1.0, and 3 m above the floor level (CL: -2.8, -2.1, -0.1 m) with 4 thermocouples attached mid-way between the toe of the flange and the web of each flange and 1 attached to the centre of the web. A total of 6 plate thermometers were also placed 0.1 m from and oriented away from the steel column to capture the incident heat flux onto the column. These were placed along the height of the column at 1.0 m, 2.4 m and 3.0 m above the floor level and on opposite sides of the column (perpendicular to the fire spread direction: Face A and Face B are oriented north east and south west respectively).

2.6.5 External flaming

Non-combustible screens were placed above one door and one window opening, located on the north east façade, to allow measurement of flame extension outside the building envelope. The façade screens were annotated with a scale to facilitate flame height and width measurements from image data recorded during the experiment. Each façade screen was instrumented with 8 thermocouples and 4 plate thermometers. The thermocouples were located above the centreline of each opening and arranged in two vertical rows, with the first row located at the façade and the second row offset by 300 mm from the façade (see Figure 5). The façade offset distance was chosen with the aim of recording the maximum external flame temperatures (i.e. on the flame centreline). The thermocouple position was established from a-priori external flaming calculations [20] and experience from the Epernon Fire Test Programme [6] and other tests.

Unlike the internal compartment thermocouples, the recorded temperature measurements from the façade thermocouples reported in this work were not corrected to account for radiation errors. Any errors resulting from radiation from the compartment fire to the façade thermocouples are expected to be small. This approach has been taken in other external flaming research [21], [22]. However, in future research focusing on assessing the external flaming from the experiment these errors could be corrected.

2.6.6 Cameras

A series of visual cameras, protected with fibreboard, were used to capture the fire size and flame spread rates. A total of 22 *Campark V20 Action* cameras were used. 12 were placed directly in the openings (Cam 1-13), but only 3 were successfully recovered (Cam 1, 2, 13). 8 cameras were installed externally to give a range of views of the compartment. Cameras 20 and 21 were positioned to observe the external flame extension from the window and door, respectively, against the non-combustible screen described earlier. While Cameras 19 and 22 gave perpendicular views of the flame extension.

Footage from all cameras, except for Cam 19 and Cam 22, were used in the image processing analysis, described in Appendix A, to measure the locations of the leading (i.e. flame front) and trailing (i.e. burn-out) edges of the fire as in *x-ONE* [11] and *x-TWO* [17]. Drones and handheld camera were also used to give a dynamic view of the fire.

2.6.7 Ambient conditions

The direction and velocity of the wind are measured before and during the test by a directional anemometer positioned 18 m to the north of the test compartment, at the same height as the ceiling. The weather conditions were calm with no detectable wind speeds. Over the first hour of the experiment the air temperature was measured to range between 2.0 – 4.6 (±1.0)°C and the relative humidity was 49% (± 5%). It should be noted that there was rainfall approximately 38.5 h after ignition.

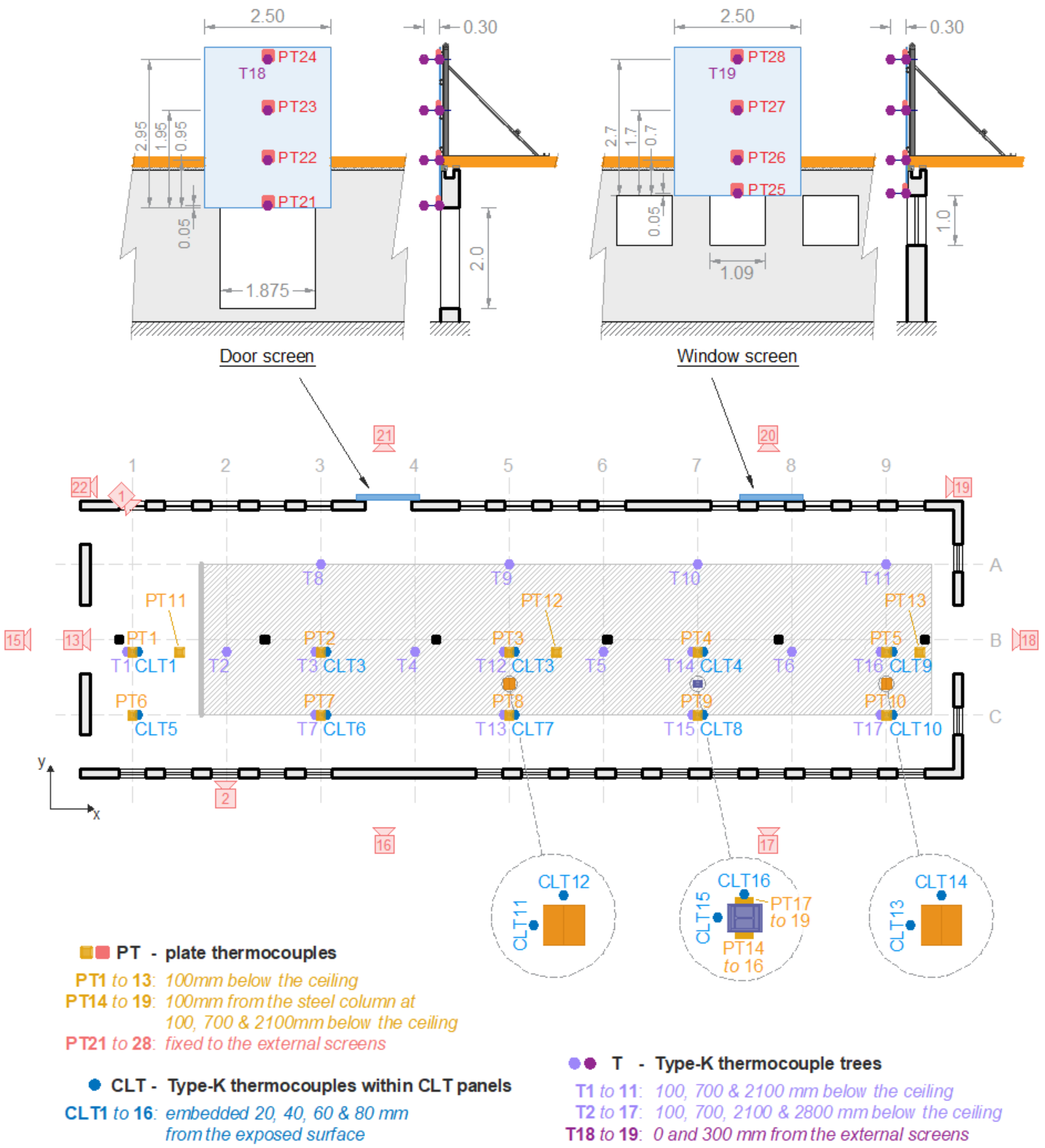

Figure 5. Overview of the instrumentation layout within the compartment, CLT ceiling, and external screens at the door and window openings.

3 EXPERIMENT RESULTS

3.1 Observations

The timeline of events is presented in Figure 6 with representative photos, while Figure 7 captures the fire development during the fire growth. Following the ignition of the methanol pans the wood crib used as fuel ignited quickly and the fire grew steadily, forming a uniform flame front across the width of the crib within 2 min. The CLT ignited shortly after at 2 min 47 s after ignition. The flames spread rapidly across the ceiling reaching the far end of the compartment within 5 min 16 s while the crib flame was more steadily progressing behind. The ignition of the CLT ceiling marked a change in the compartment fire dynamics. Shortly after the ignition and spread of flames across the CLT, the crib flames accelerated across the length of the compartment and reached the far end of the crib at 5 min 36 s after ignition. It appears that the spread along the crib was enhanced by the radiative heating from the burning CLT as the surface of the crib was seen to ignite (see 4 min 20 s in Figure 7).

Flame extensions, between 0.5 and 1.5 m above the window and door opening soffit, were observed locally through 3 window openings on either side near the ignition and the north west entrance shortly after the CLT ceiling had ignited (see 3 min 40 s, Figure 7). Similar small external flaming was observed from windows where the flame had spread over the CLT. This was intensified by the arrival of the flames which spread along the crib. Once the crib fire had reached the far end of the compartment, extensive external flaming was visible from all windows with flames up to ~3 m in height (see Section 3.8 for further details). After approximately 12 min flame extensions were localised to the far end of the compartment, with minimal flaming (predominately emanating from the flaming CLT) through the openings near the ignition side. The CLT appeared to burn consistently beyond the extent of the burning crib, even while the fire size of the crib decreased. The flaming of the CLT receded from the ignition end of the CLT towards the far end of the compartment, until the complete cessation of flaming combustion of the exposed CLT surface at approximately 17 min 30 s after ignition. At this time, the flames from the crib had diminished in size, no longer impinging on the ceiling, and were limited to the area between 12.2 m and 19.7 m from the ignition location. The flaming of the crib ceased 22 min 30 s after ignition, but the remaining embers continued to smoulder for approximately another 37 min. The internal walls of the compartment were seen to be nearly completely clean from soot, which may suggest a well ventilated and fuel-controlled fire.

Following the end of flaming in the compartment some hotspots in the CLT where observed, although the majority of the CLT had stopped burning as it was observed visually and via thermal imaging cameras. The morning after the experiment, approximately 12 h after ignition, four hotspots were detected via thermal imaging camera and visual detection of smoke and spontaneous transition to flaming (see ~12 h in Figure 6). One hotspot near the central concrete beam continued to burn, eventually burning a hole through the thickness of the CLT slab. This hole widened over the course of the day until rainfall extinguished the smouldering approximately 38.5 h after ignition of the wood cribs, before full smouldering extinction at 40 h. This smouldering behaviour of the CLT is discussed further in Section 3.7.

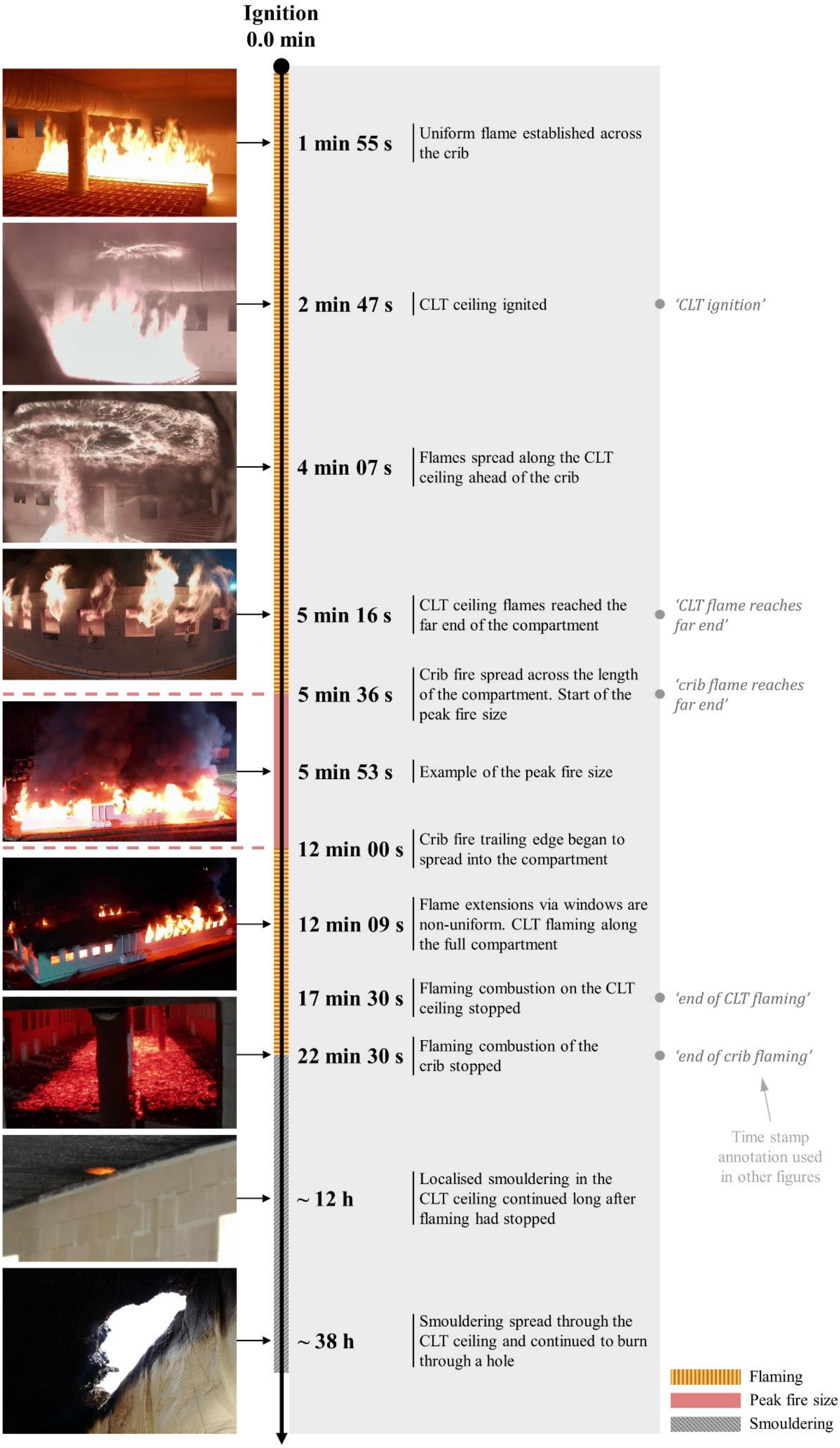

Figure 6. Timeline of the experiment, presenting the key events and representative photos.

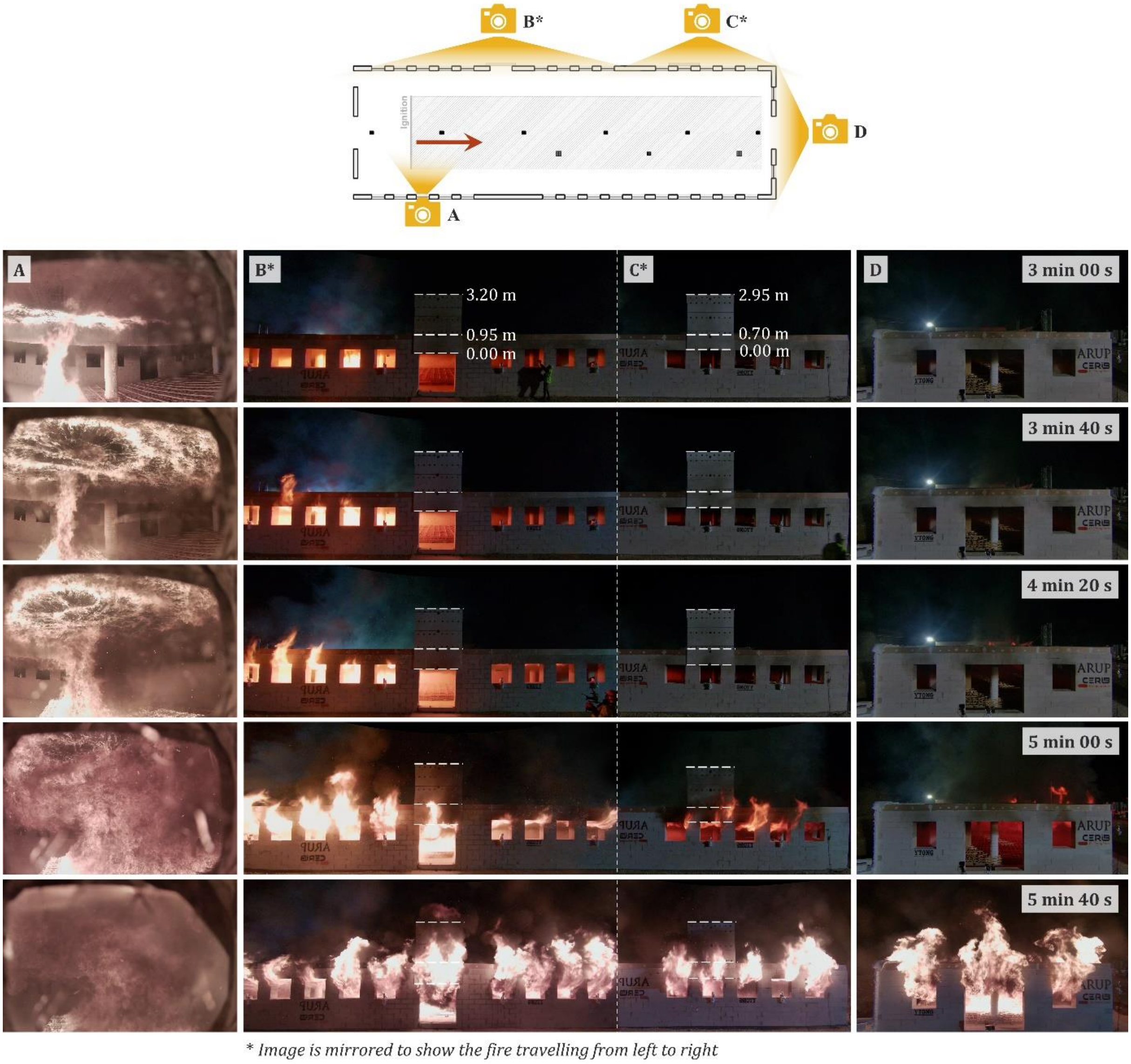

Figure 7. Images capturing the growth stage of the fire from just after the ignition (2 min 27 s) of the CLT to just after when the crib flames have travelled the length of the crib (5 min 36 s). Images from camera positions B and C have been combined together to give a continuous view of the compartment and mirrored to show the fire travelling from left to right. The dotted vertical white line marks where the images are merged. The horizontal dashed white lines note the height of the external screens above the openings.

3.2 Leading and trailing edges

Using the visual footage of the fire (from fixed and drone mounted cameras), the spread of flame across both the crib and CLT was observed and measured. The leading edge is defined by the foremost location of burning on the ceiling or fuel bed respectively, while the trailing edge is characterised by the location at which the flame has reduced in size to a point where the fuel no longer has continuous visible flaming combustion.

Location and spread rates of the leading and trailing edges with time for both the crib and CLT are extracted from the visual evidence and observations taken during the experiment and illustrated in Figure 8. The fire on the CLT, in addition to spreading in the same direction as the crib fire (to the south east – noted in Figure 8 as forward), it also spread in the opposite direction (towards the north west entrance – noted in Figure 8 as backward). Lines for the leading and trailing edges represent best fit curves for each set of data.

The flame spread along the crib was observed to be steady in the early stages of the experiment (11 mm/s), but accelerated across the compartment shortly after the ignition of the CLT. The leading edge was also observed to regress into the compartment as the crib at the far end of the compartment was consumed. This may be due to the increased burning rate facilitated by the large door opening to the south east providing ample oxygen supply. The trailing edge, was identifiable and began to traverse the compartment at approximately 12 min and steadily spread across the compartment with an average spread rate of 37 mm/s. The distinct and identifiable movements of both the leading and trailing edge are characteristic of a travelling fire.

The flames spread rapidly across the CLT ceiling once it was ignited, heating and igniting a greater region of the ceiling which in turn spread the flame further along the ceiling. The CLT flaming extended beyond the extent of the crib as evidenced by the flaming of the CLT before the ignition location and continued flaming after the movement of the trailing edge from the same area. The average spread rate of flames across the CLT, based on the time between the ignition of the CLT and the flames reaching the far end of the compartment, was 200 mm/s spreading 30 m in 2 min 29 s.

Fire was at its maximum size between 6 and 12 min when the full extent of the crib and CLT were burning simultaneously. This uniform burning may be caused by the rapid spread of the fire across the ceiling throughout the whole compartment and radiating to the fuel below. Therefore, it is representative of typical flashover behaviour in classic non-combustible compartments when rapid ignition of all fuel takes place due to the radiation from the accumulating smoke layer when it reaches average temperatures of 450 - 670°C [9] but in *CodeRed #01* it was driven by direct radiation from flames at the ceiling

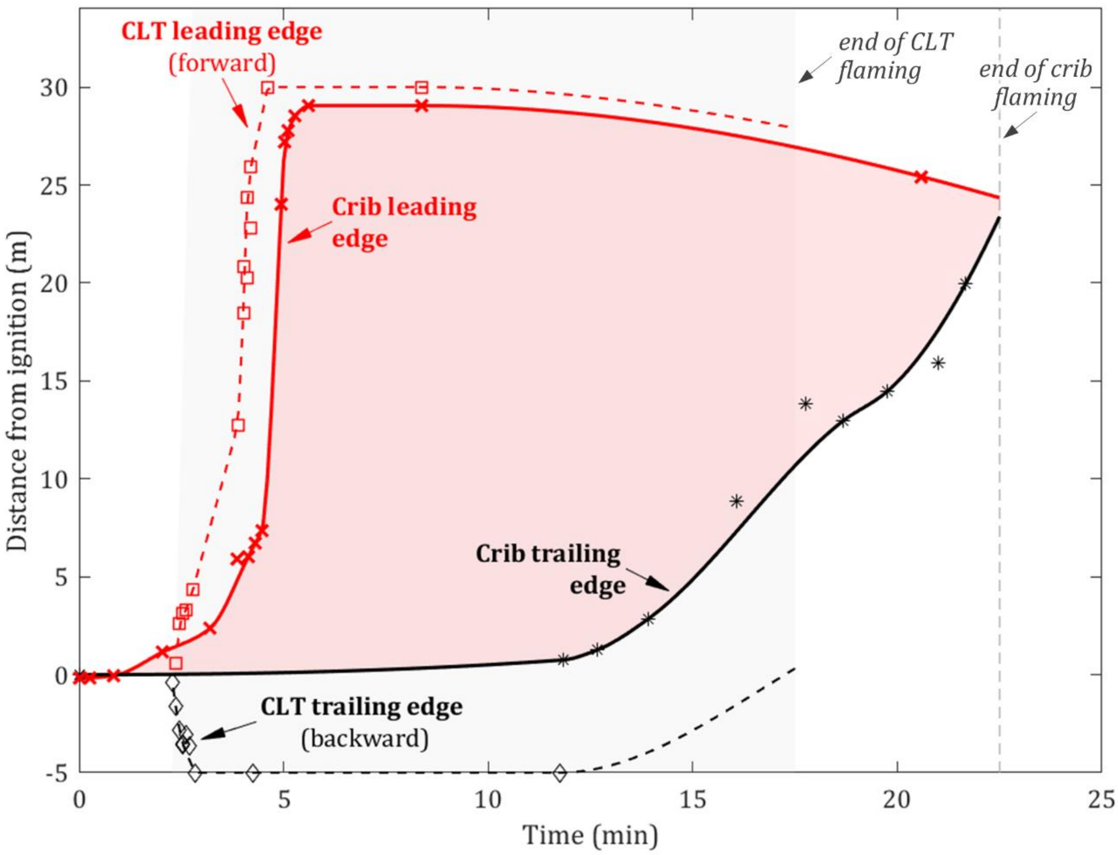

Figure 8. Locations of the leading and trailing edges of flame spread across the CLT (dashed lines) and the wood crib (solid lines). The time of end of observed flaming combustion of the CLT (17.5 min) and crib (22.5 min) are marked with vertical shaded area and dotted line, respectively.

3.3 Heat release rate

The HRR was calculated following the method established for x-ONE [11] and also used in x-TWO [17], which considers the fuel load, local burning duration, combustion efficiency of 0.7, and uses the fire spread data from the image processing as visual evidence. Separate HRR were calculated for the wood crib, CLT, and both glulam columns before being summed to give the total HRR as presented in Figure 9. The HRR for the CLT ceiling was calculated using the same methodology as for the crib but utilised the weighted average char depth profile along the compartment to determine the fuel load distribution. The weighted average char depth profile was based on measurements taken from saw cuts made through the CLT panels after the experiment (see Section 3.6) and weighted based on the lateral distance between char depth measurements. The full extent of the CLT ceiling was assumed to burn until the end of CLT flaming combustion. HRR for the glulam columns was similarly based on the measured char depth and was assumed to ignite and extinguish following the arrival of the leading and trailing edge of the crib fire, respectively.

The peak HRR achieved in this period was estimated to be in the order of 121 MW. The peak HRR of the crib was approximated to be 61 MW, while the CLT ceiling was estimated to contribute 60 MW. Glulam columns 1 and 2 contributed 0.17 and 0.20 MW respectively.

Comparing the fire growth rate to standard t^2 fires, the HRR grew more rapidly than an "ultra-fast" fire growth rate, noting this comparison is made only for context and that these curves are not representative of compartment fires. The average heat release rate over the course of the fire was 99 MW.

Integrating under the HRR curve of the CLT and correcting for the applied combustion efficiency gives a fuel load of 71,200 MJ. Comparing this to the approximate 65,100 MJ of fuel in the wood crib, shows an approximate equal contribution of energy from the CLT as from the wood crib. It should be noted that the CLT fuel load is based on the final char depth measurements at the end of the experiment. No correction could be made to discount the amount of char that was produced after the end of flaming. However, the temperatures measured at 20 mm depth from the surface of the CLT reached their peaks around 40 minutes after ignition, suggesting that smouldering after the fire may not have been significant across the majority of the compartment. No loaded or unloaded material testing was undertaken of the samples collected after the fire.

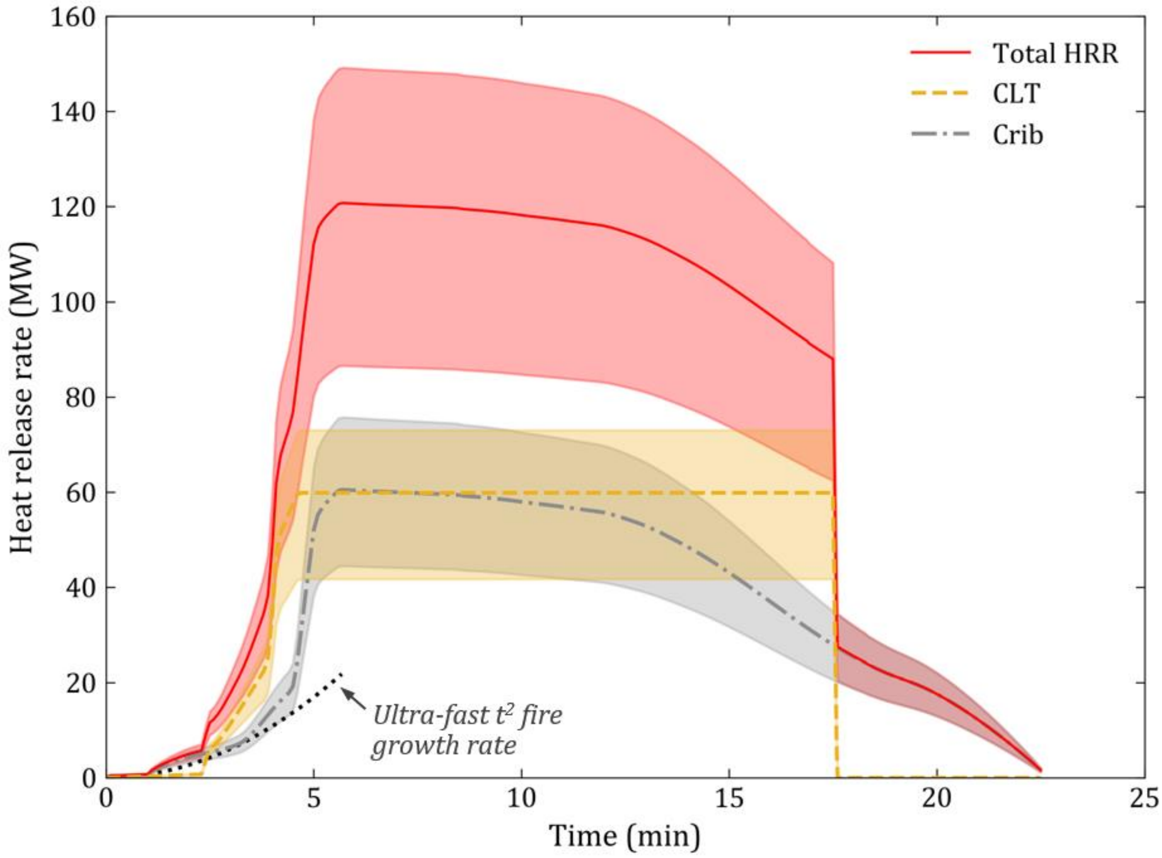

Figure 9. Calculated individual and combined (total HRR) heat release rates of the wood crib and CLT. Glulam column 1 and column 2 contribute peak HRRs of ~0.17 MW and ~0.20 MW respectively but are not plotted here. The cloud error bars capture uncertainty in assumed combustion efficiency (0.60-0.75), variations in CLT char depths, and fuel load density. The ultra-fast standard t^2 fire growth rate is provided for comparison.

3.4 Gas phase temperatures

Figure 10 presents the temperature profiles of the thermocouples 0.35 m offset from the centreline of the compartment, near the ceiling (FL: +3.0 m, CL: -0.1 m) and above the crib (FL: +1.0 m, CL: -2.1 m). The temperature near the ceiling increased up to approximately 300°C in the early stages of the fire growth as smoke traveled down the compartment (Figure 10A). The CLT ignited at 2 min 46 s, resulting in a significant temperature increase in the thermocouples closest to the ignition location (T1 and T3). The flame spread rapidly across the CLT reaching the other end of the compartment at 05 min 16 s, ahead of the crib fire. During this time the temperatures near the ceiling grew rapidly up to a peak temperature of 1030°C. Figure 11 presents the temperature distribution by showing a vertical cross-section through the centreline of the compartment at various times, along with images from outside the compartment. The top image and plot of Figure 11 presents the temperature data shortly after the flame on the CLT had spread the length of the compartment, as indicated by the elevated temperature near the ceiling and the associated image. The temperature near the crib then rapidly increases on the arrival of the crib flame. As such, the temperature near the crib (FL: +1.0 m, CL: -2.1 m) shows a characteristically different temperature profile compared to the temperatures near the ceiling (FL: +3.0 m, CL: -0.1 m) as it did not experience gas temperatures above 150°C until the arrival of the flame (Figure 10). Shortly after the flame had spread across the full length of the crib (5 min 36 s) all thermocouples reached an approximate steady state, at around 1000°C, except for the thermocouples in T1 which are located before the start of the wood crib which reached around 800°C.

During the decay phase of the fire, gas temperatures steadily decreased from peak temperatures to less than 100°C over 53 min after the end of peak flaming (which occurred between 6 to 12 min after ignition). The cooling phase is also notably different between the thermocouples near the ceiling and above the crib. The ceiling gas temperatures appear to cool uniformly (Figure 10B) while the gas temperature 1 m above the floor level is staggered with lower temperatures towards the ignition end of the compartment. This is likely due to the difference in the flaming behaviour of the CLT and the crib. A clear trailing edge was observed on the crib, travelling along the compartment as the fuel was consumed, the flaming of the CLT on the other hand extinguished nearly simultaneously across the length of the compartment, resulting in the near ceiling temperatures to cool more uniformly while lower in the compartment cools sequentially. This is also visually apparent as the gas temperatures near the ceiling quickly decrease following the end of CLT flaming (Figure 10B).

The maximum lateral temperature variation, as measured by comparing the maximum temperature differences between the thermocouples near the centreline of the compartment and over the edge of the crib along the compartment, broadly remained less than 100°C for gas temperatures measured at FL +2.4 m and +3.0 m. This was largely independent with distance along the compartment, with exception for the thermocouples on gridline 3, positioned 1 and 2.4 m above the floor level. The average maximum lateral temperature variation taken over the peak burning duration (between 6-12 min) was 311 and 133 °C at 1 and 2.4 m above floor level respectively.

However, more significant variation in temperature existed when comparing across the length of the compartment. The maximum temperature difference between any two thermocouples was found to be 990°C during the growth stage. While the average maximum temperature variation during the steady state stage was 673°C across all thermocouples, and 517 °C when considering only thermocouples where the crib was constructed (i.e. excluding T1), clearly illustrating the non-uniformity of temperatures within large compartments.

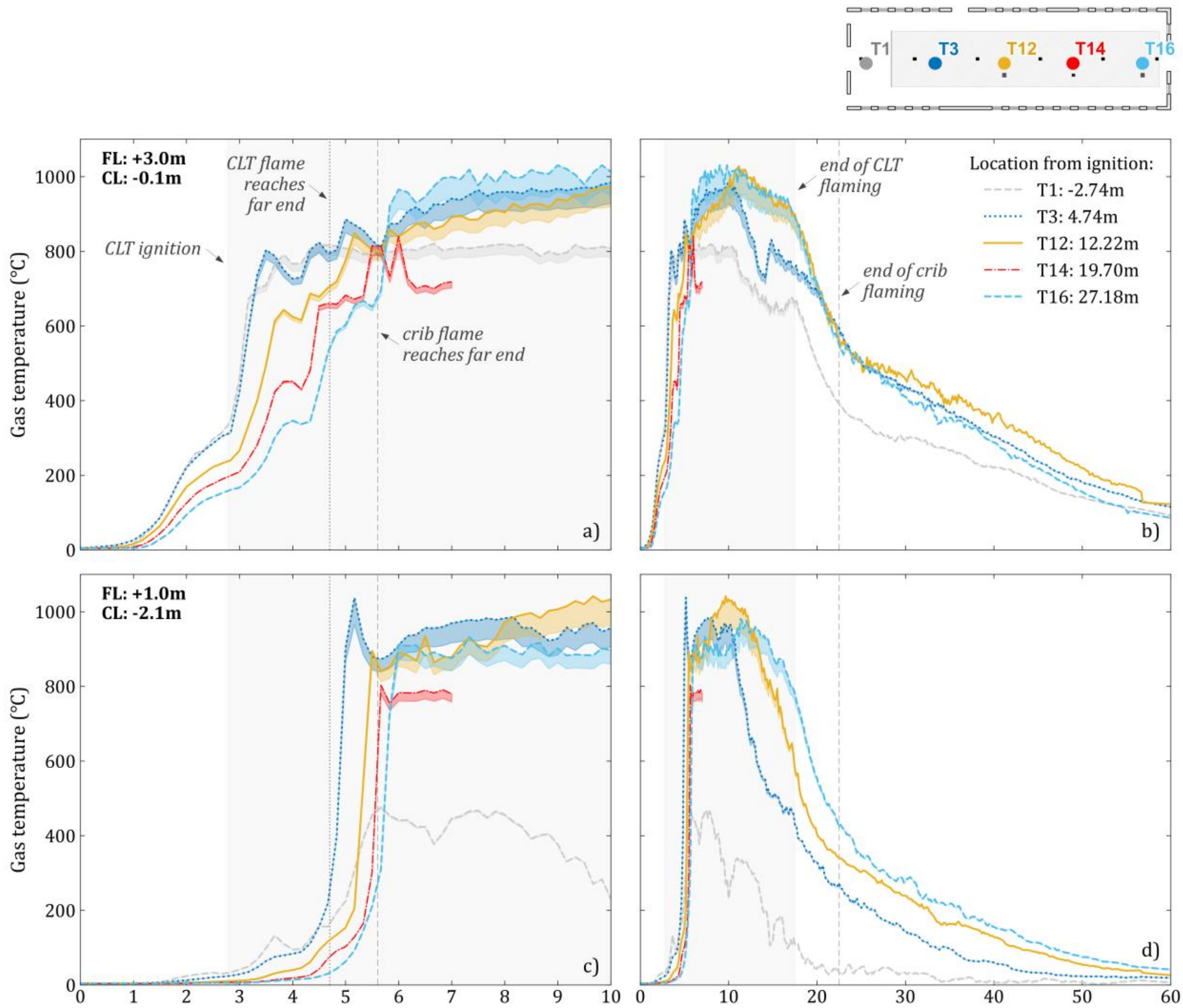

Figure 10. Gas temperatures along the centreline measured at +3.0 m above floor level = - 0.1 m below ceiling level (a) and b)), +1.0 m above floor level = -2.1 m below ceiling level (b) and c)). Shown during the first 10 min (a) and c)) and 60 min (b) and d)) after ignition. Shaded clouds represent uncertainty in the thermocouple. T14 failed after 7 min, and so only data before this is shown.

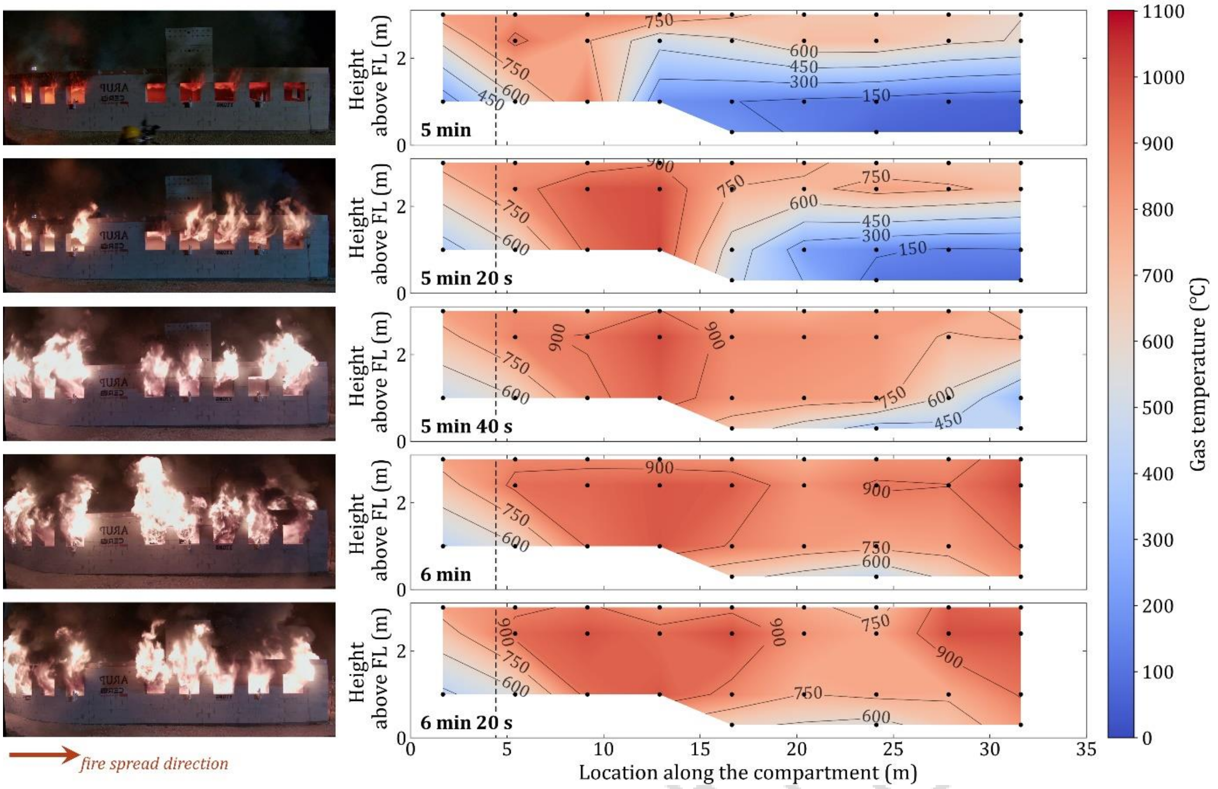

Figure 11. Vertical temperature distribution along the centreline of the compartment presented at various times from 5 min (top) to 6 min 20 s (bottom) after ignition. Black dots indicate location of thermocouples, while the black dashed line indicates the ignition location. The photographs are from camera 20 and give a visual of the compartment fire at the time of the adjacent contour plot. The photographs are mirrored to show flames moving from left to right.

The comparison between the vertical temperature profiles at various positions along the centreline of the compartment is shown in Figure 12. As in Figure 10 and Figure 11 the temperature near the ceiling increases first (FL: +3.0 m, CL: -0.1 m), followed sequentially by the lower thermocouples. However, this changes after ~5 min whereby the greatest temperatures (1060 °C) are measured by the thermocouple located at FL +2.4 m, while the gas temperature near the ceiling is slightly lower (reaching up to 1030°C). This was similarly reported by Gorska et al [23] who conducted experiments in timber compartments measuring 0.50 (width) × 0.50 (length) × 0.37 (height) m suggesting that compartments with combustible linings do not experience much of a thermal gradient through their height. Non-combustible compartments, on the other hand, typically result in temperature gradients through the height, with the highest gas temperatures near the ceiling [11], [17].

For *CodeRed #01* the mid height (FL: +2.4 m, CL: -0.7 m) temperatures dropped below that near the ceiling sequentially with distance: 8.5, 11.5, and 14.5 min after ignition at T3 (4.74 m), T12 (12.22 m) and T16 (27.18 m) respectively. Following this, the temperatures near the ceiling remain hotter (by up to 200°C) compared to lower in the compartment due to continued flaming of the CLT ceiling and the decreasing fire size of the crib. The difference in temperature with height decreased with distance from the ignition location because the CLT, as discussed earlier, was observed to extinguish nearly simultaneously, while the crib burned out progressively along the compartment (marked by the trailing edge) causing a greater time difference between the local burn out of the CLT and the crib.

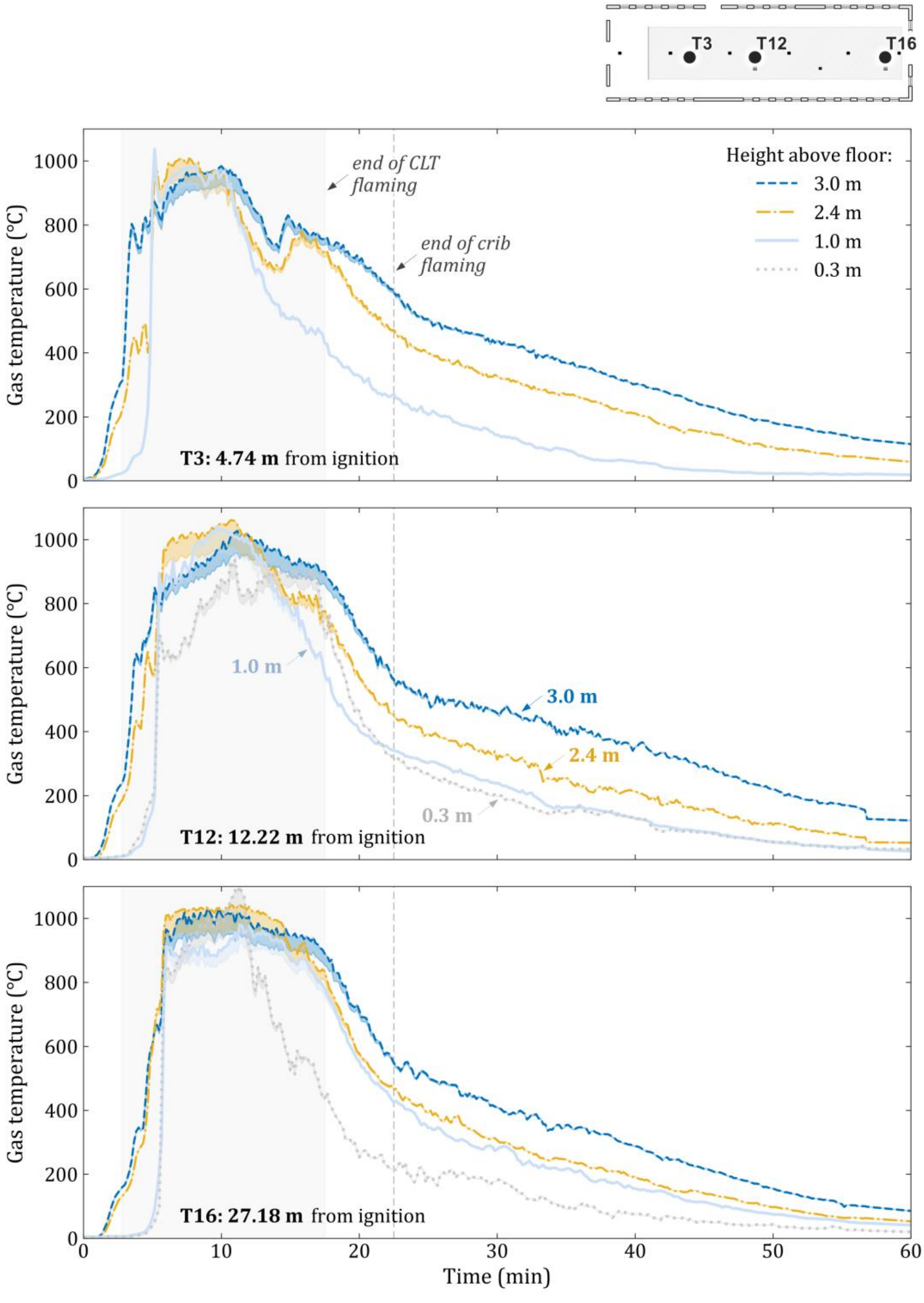

Figure 12. Vertical temperature variation within the compartment at 3 locations along the centreline: 4.74 m, 12.22 m, and 27.18 m from ignition. Shaded clouds represent uncertainty in thermocouple data. T14 (between T12 & 16) failed and no thermocouple was positioned at 0.3 m above floor level at T3 and, thus, they are not presented here.

3.5 Incident heat flux

The incident heat fluxes were calculated by converting the temperatures measured by the plate thermometers mounted near the centreline of the compartment as well as along the perimeter of the crib in accordance with the method used by Ingason and Wickstrom [24] and Bystrom et al. [25] using eq. 2 below:

$$\dot{q}''_{inc} = \sigma T_{PT}^4 - \left((h_{PT} + K)(T_g - T_{PT}) - C\frac{dT_{PT}}{dt} \right) \tag{2}$$

where σ is the Stefan Boltzmann constant, T_{PT} is the temperature of the plate thermometer, h_{PT} is the coefficient of heat transfer on the plate (11 W/m^{2}K [25]]), K is the conduction coefficient (8.34 W/m^{2}K [25]), T_g is the gas temperature around the plate thermometer, and C is the heat capacity of the plate thermometer (4202 J/m^{2}K [25]).

The incident heat flux as measured by the plate thermometers at 0.1 m below the ceiling along the centreline of the compartment is presented in Figure 13. The maximum heat flux reached was 270 kW/m^2 towards the centre of the compartment. The lateral variation in heat flux, varied by up to 75 kW/m^2 equating to a 35 % decrease from the centreline heat flux. The average variation in heat flux during the peak burning period was found to be roughly consistent with distance along the compartment ranging between 17 to 44 kW/m^2 with the heat flux being greater near the centreline when compared to the edge of the crib. The exception was near the north west entrance where there was no crib built, which showed an average lateral variation of less than 5 kW/m^2 during the peak burning period.

The vertical variation of heat flux is shown in Figure 14. Plate thermometers were mounted at three heights (1.0, 2.4 and 3.0 m above the floor level) along the steel column located 19.7 m from ignition, and on two sides of the column: facing inwards into the centre of the compartment (Face A) and facing outwards, towards the window openings (Face B). The highest heat flux was measured by the plate thermometers on Face B, which reached a peak of 310 kW/m^2, while Face A reached 260 kW/m^2. The higher heat flux on Face B may be due to the oxygen supply from the window opening allowing for improved combustion. On both faces the peak heat flux is measured by the middle plate thermometer at 2.4 m above the floor level, with the peak heat flux near the ceiling being the smallest reaching 215 and 227 kW/m^2 for Face A and B respectively. This is the same behaviour as was found for the gas temperatures (Figure 12). The peak heat fluxes measured near the ceiling are seen to be similar on both sides of the column and similar to those measured along the centreline.

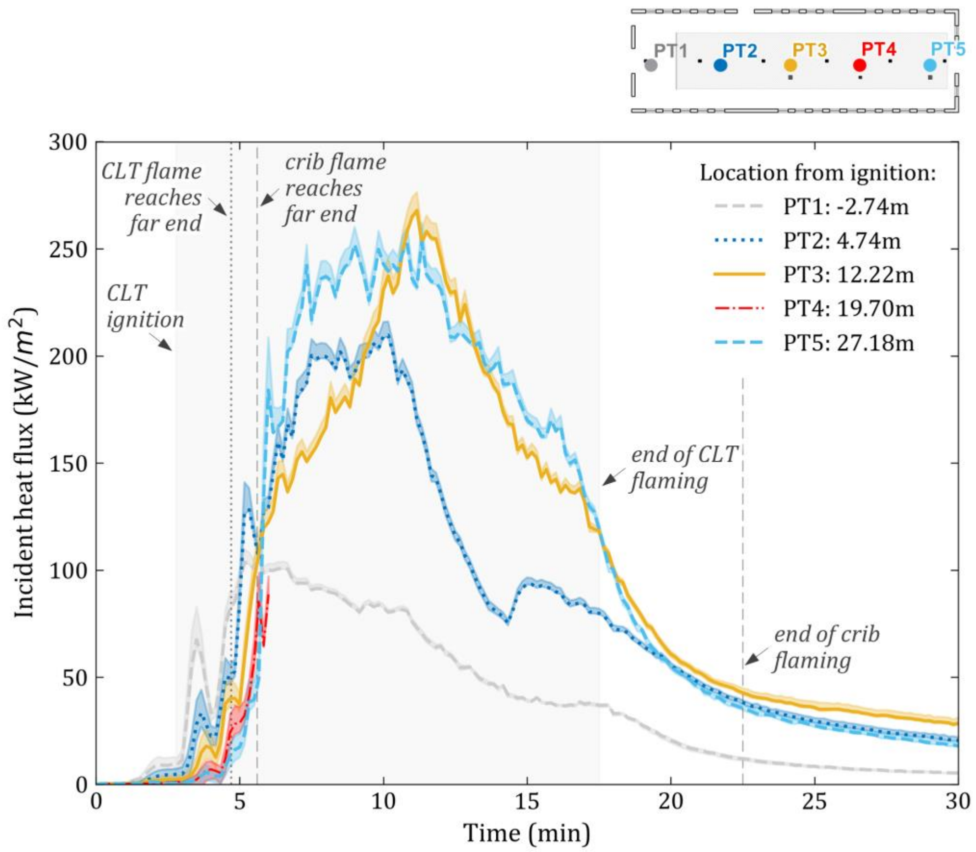

Figure 13. Incident heat flux along the centreline of the compartment measured at +3.0m above floor level (FL) = -0.1m below ceiling level (CL). Shaded clouds represent the maximum and minimum heat fluxes of all permutations of emissivity = 0.7 to 0.9 [26]; coefficient of heat transfer=5 to 25 W/m^{2}K [9], and uncertainty in thermocouple data. PT4 failed after 7 minutes and, thus, only data capture before this is presented.

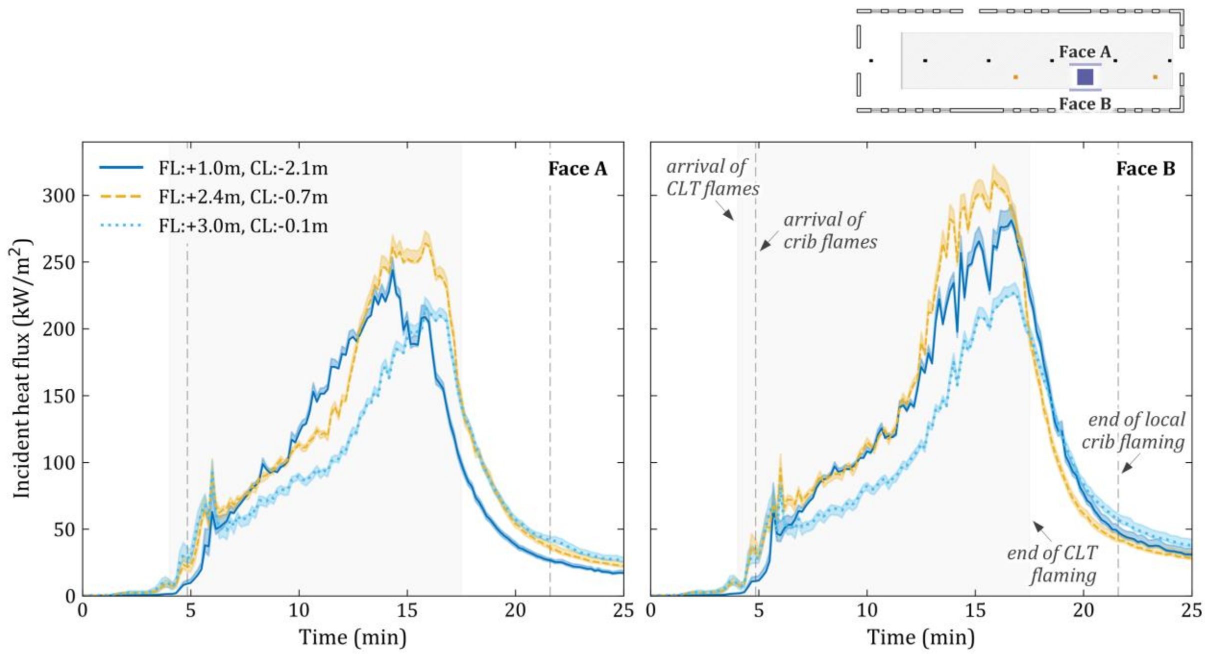

Figure 14. Heat fluxes along the height of the steel column, located 19.7 m from ignition. Face A is inward, facing the centre of compartment, while Face B is on the side of the column

facing the wall and openings (outward). Shaded clouds represent the maximum and minimum heat fluxes of all permutations of emissivity =0.7 to 0.9; coefficient of heat transfer=5 to 25 W/m^{2}K [9] and uncertainty in thermocouple data.

3.6 CLT ceiling and glulam column performance

In this section the performance of the CLT ceiling and glulam columns are reviewed at high level. A detailed review of the structure and the potential impact on structural response will be investigated in future work as it is outside the scope of the current paper due to its focus on the compartment fire dynamics.

CLT Ceiling

The pyrolysis and thermal penetration depth in the 140 mm CLT panels was measured through in-depth thermocouples and post-test saw cuts through panels, refer to Section 2.6.3 for details.

Temperatures recorded within the CLT panels are shown in Figure 15. These indicate that at 20 mm from the exposed surface, the temperatures in the panels were in a range of approximately 100°C to 200°C for around 80 minutes. Temperatures at 40 mm depth were generally well below 100°C. It should be noted that as the thermocouples were inserted from the back the temperatures measured here are expected to underestimate the temperature within the timber due to conduction via the metal thermocouples as explained by Pope et al. [19]. Pope et al. [19] in samples of laminated bamboo found temperatures measured from the back to underpredict temperature measured from the side (parallel to the isotherm) by up to 60% for the range of temperatures of interest to this work. This aspect is intended to be examined more closely in a future publication, and explains why the thermocouples do not reach pyrolysis temperatures despite the average char depth exceeding 20mm in the postfire inspections.

The transient thermal penetration can be seen within Figure 15, where the peak temperatures are observed to occur well after the end of flaming which is noted with a vertical line. On average the peak temperatures were reached 36, 50, 106, and 171 min after ignition for 20, 40, 60, 80 mm respectively. This transient thermal lag will be studied further in the future publications given the importance to residual load-bearing capacity of timber members.

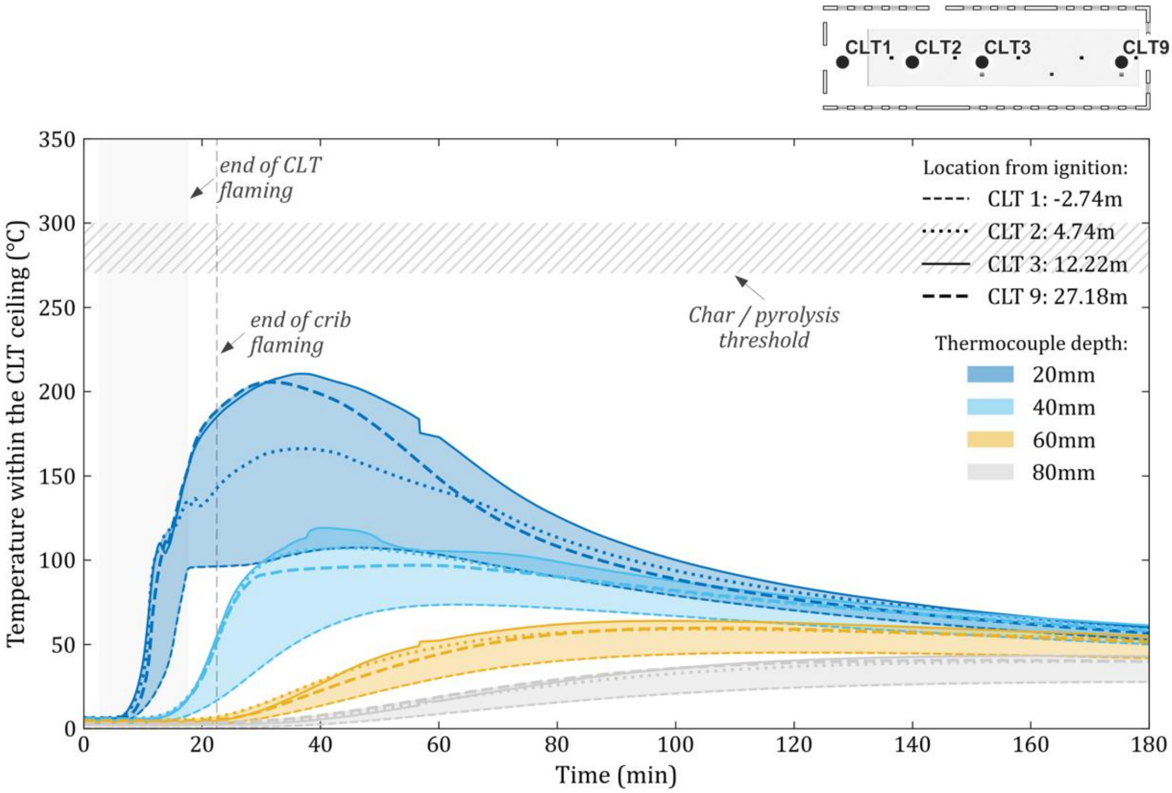

Figure 15. In-depth CLT thermocouple measurements along the compartment (0.375 m from the centreline to the South West). Shaded areas represent thermocouples positioned at the same depth from the exposed surface of CLT.

To determine the actual char depth at the end of fire exposure, saw cuts were made at similar locations to the thermocouple groupings. The cuts were taken a few days after the experiment was completed. At each saw cut, measurements were carried out and photographs taken of the residual cross-section. Distance measurements from the unexposed face to the char layer were taken at several location along each cut and averaged. The char depth was then found by subtracting the measured depth from the original section depth to give the char depth. The weighted average depth of charred timber across the entire ceiling was 25.4 mm, weighted by distance between measurements along the compartment and laterally.

Figure 16 shows char depth estimated from the saw-cuts of the CLT samples located near the building centreline, with depths recorded along the building length. The smallest average char depth (18 mm) was measured above the region where no crib was constructed. However, above where the crib was constructed a slight increase in char depth with distance was found: with an increase of 10% from 29 mm, 4.34 m from ignition, to 32 mm, near the south east entrance, 31.29 m from ignition. This is likely due to the longer exposure to flames and radiant heat of the CLT at the far end of the building.

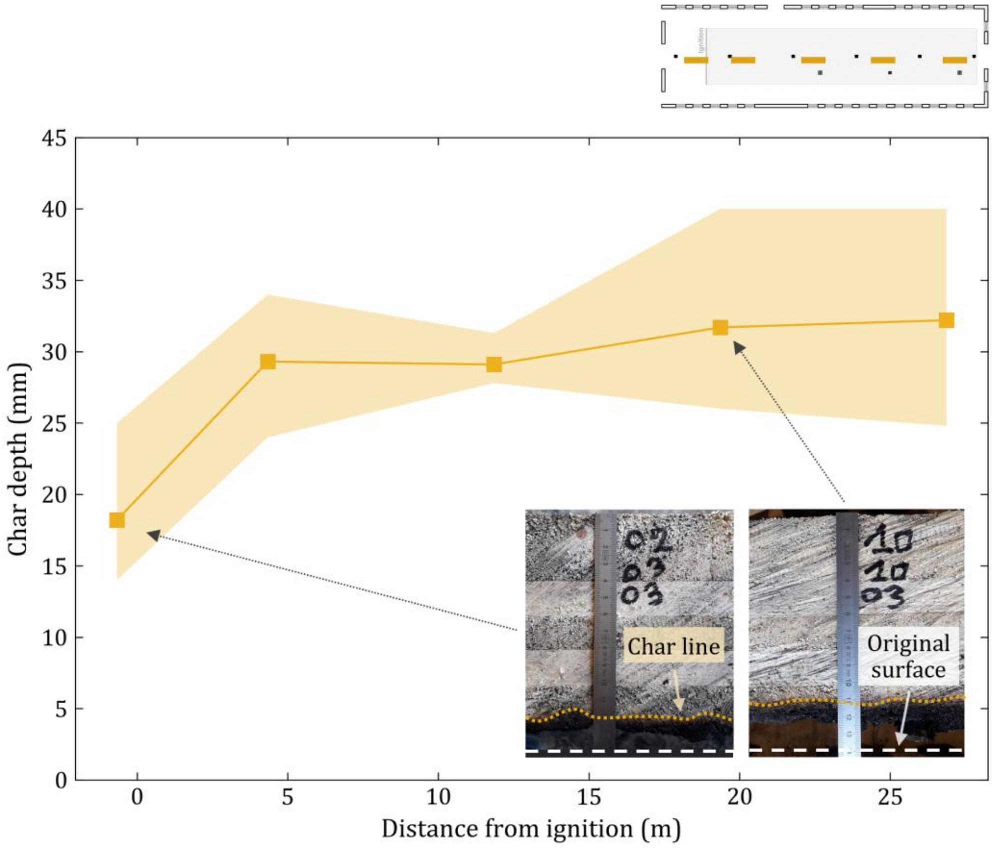

Figure 16. Post fire char depths measured from residual cross-sections for selected CLT panel samples along the compartment length, located near the building centreline. Diagram at the top indicates locations of the panel section cuts. The shaded cloud represents the minimum and maximum char depth measured along a cut.

Glulam Columns

Glulam column temperatures at 20 mm depth from the exposed surface at three differing heights are shown in Figure 17. Temperature readings in both columns show a clear difference in temperatures between the two faces where thermocouples were located, with the thermocouples facing into the compartment (Face A) recording significantly higher temperatures than those facing the windows (Face B). On average the peak temperature reached on Column 1 was 533 and 319 °C and for Face A and B on respectively, while Column 2 reached 554 and 443°C respectively.

In contrast, the protected steel column was measured to have a higher incident radiative heat flux on Face B than on Face A (see Section 2.6.4). As such the explanation of the higher temperature on Face A, compared to Face B, in the timber columns may be due to the relatively lower total heat flux received on column Face B. As the radiative heat flux was measured to be greater on Face B than on Face A, this may suggest that Face B experiences lower rates of convective heat transfer. This in turn may be due to differing fluid dynamic condition between the two faces as hot gasses move towards the openings.

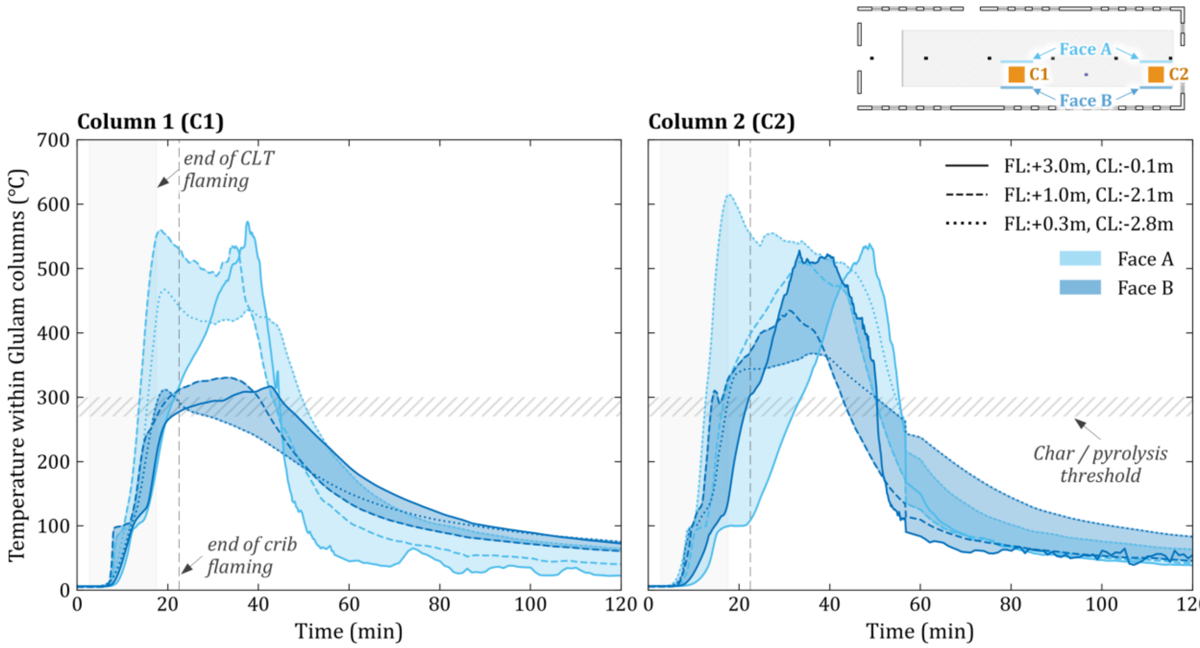

Figure 17. Recorded thermocouple temperatures at 20mm depth from the exposed surface in glulam column 1 and column 2 at heights of approx. 3 m, 1 m and 0.3 m above the floor in Face A and Face B. Vertical thermocouple positions in Face A are 6 cm lower than in Face B.

The thermal penetration lag within the glulam columns was also observed with peak temperatures in the occurring up to 26 minutes after the end of flaming combustion in the compartment. As in the CLT, the lag is more pronounced at deeper locations. The thermal penetration lag is undergoing further assessment and is planned to be presented in future publications.

To study the char depth profile along the height of the timber columns, cuts through the column were made at 3 locations near the thermocouples. Images were then taken of the cuts and at the base and top of the column (five locations in total) for each column the residual cross-sections were measured. The average char depths for both columns at varying heights above floor level are shown in Figure 18. The average char depth for column 1 and 2 was 30.2 and 30.4 mm respectively. This was calculated by using weighted average based on the distance between measurements on the average char depth measured at each height above the floor level.

Little difference can be observed when comparing the two columns, implying that position within the compartment had little impact on the charring. Also, in both cases the char depth can be seen to be largely consistent with height. The weighted average char depth of the top and bottom 0.3 m of the column is 27.8 and 30.3 mm for column 1 and 2 respectively. The middle 2.5 m had a weighted average char depth of 30.6 and 30.4 mm for column 1 and 2, respectively. However, a greater variability in char depth are measured near the base than elsewhere on the column. This may be due to prolonged heating from smouldering embers facilitating continued smouldering combustion. As this may have significant structural implications it deserves further study. A small increase in charring at the top of the column in relation to the middle of the column is also noted that is likely due to the additional burning at the ceiling.

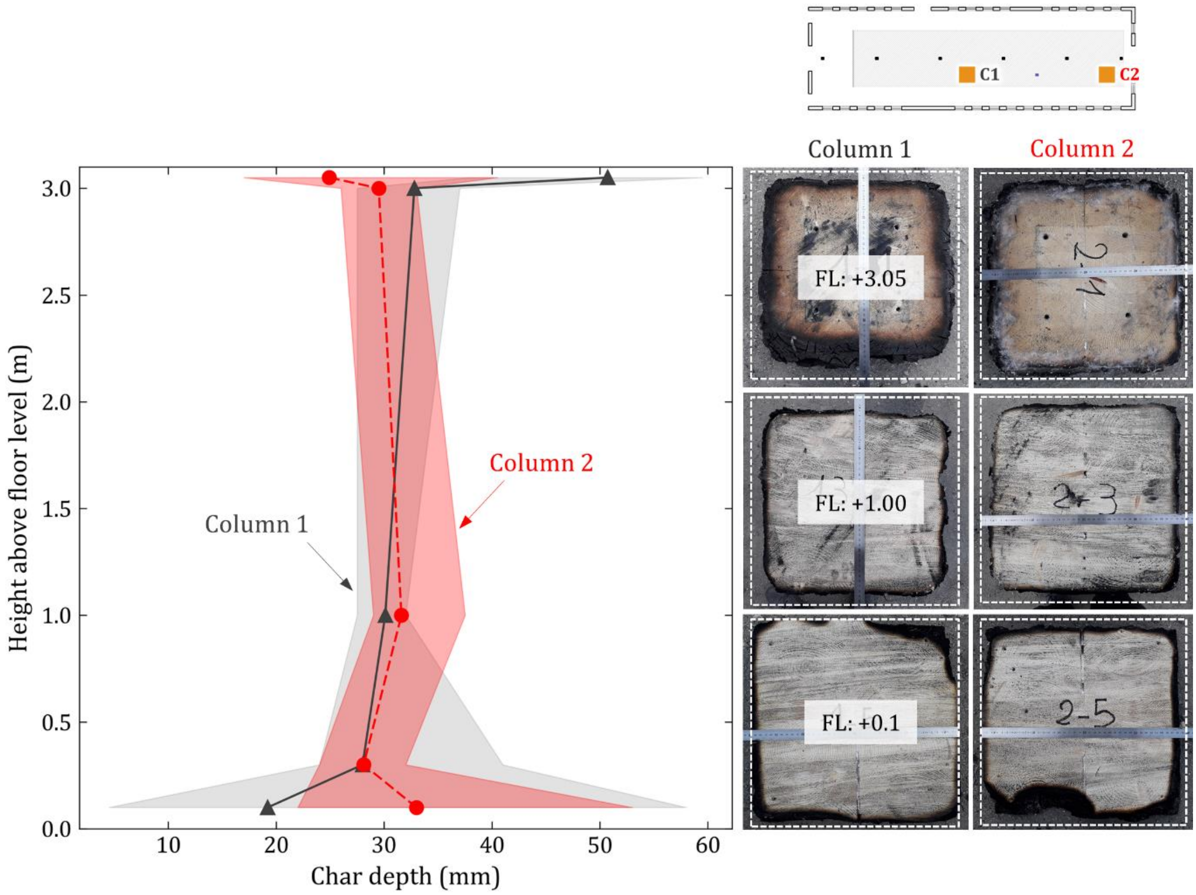

Figure 18. Averaged char depth profile of glulam columns with height above the floor level measured from residual cross-section data taken after the end of fire. Shaded clouds show the minimum and maximum char depths measured at each height. Images of the cross-sectional cuts used to measure char depth of both Column 1 and Column 2 are provided on the right. Images present cuts at 3.05 m (top), 1.0 m (middle) and 0.1 m (bottom) above the floor level. The white dotted box indicates an approximate original surface position.

3.7 Decay and Smouldering

The flaming combustion of the CLT stopped approximately 3 min before the end of the flaming combustion of the wood crib, after which the CLT char surface continued to glow, indicating smouldering combustion within the CLT slab. Following the cessation of flaming combustion of the crib, the glowing of the CLT became quickly localized to the area between 12.2 m and 19.7 m from the ignition location. Within an hour after ignition (38 min after the cessation of flaming combustion of the crib), glowing of the CLT was no longer visible.

The peak CLT temperature of 210°C at 20mm depth was measured 38 minutes after ignition (around 20 min 30 s after the end of all flaming) due to thermal lag. The latter peak CLT temperature refers to CLT thermocouples located in the compartment (away from glulam columns). All embedded ceiling thermocouples dropped below 100°C, 79 min after the end of flaming, as indicated in Figure 15. However, several smouldering hotspots on the CLT ceiling were observed over a two-day period after the experiment. They occurred at four localised regions (visible in the infrared images in Figure 19): at the junction of the CLT with the compartment wall (two cases), along the centre of CLT panels at the junction with the insulated concrete support beam (two cases, with the most significant occurring towards the ignition end of the compartment).

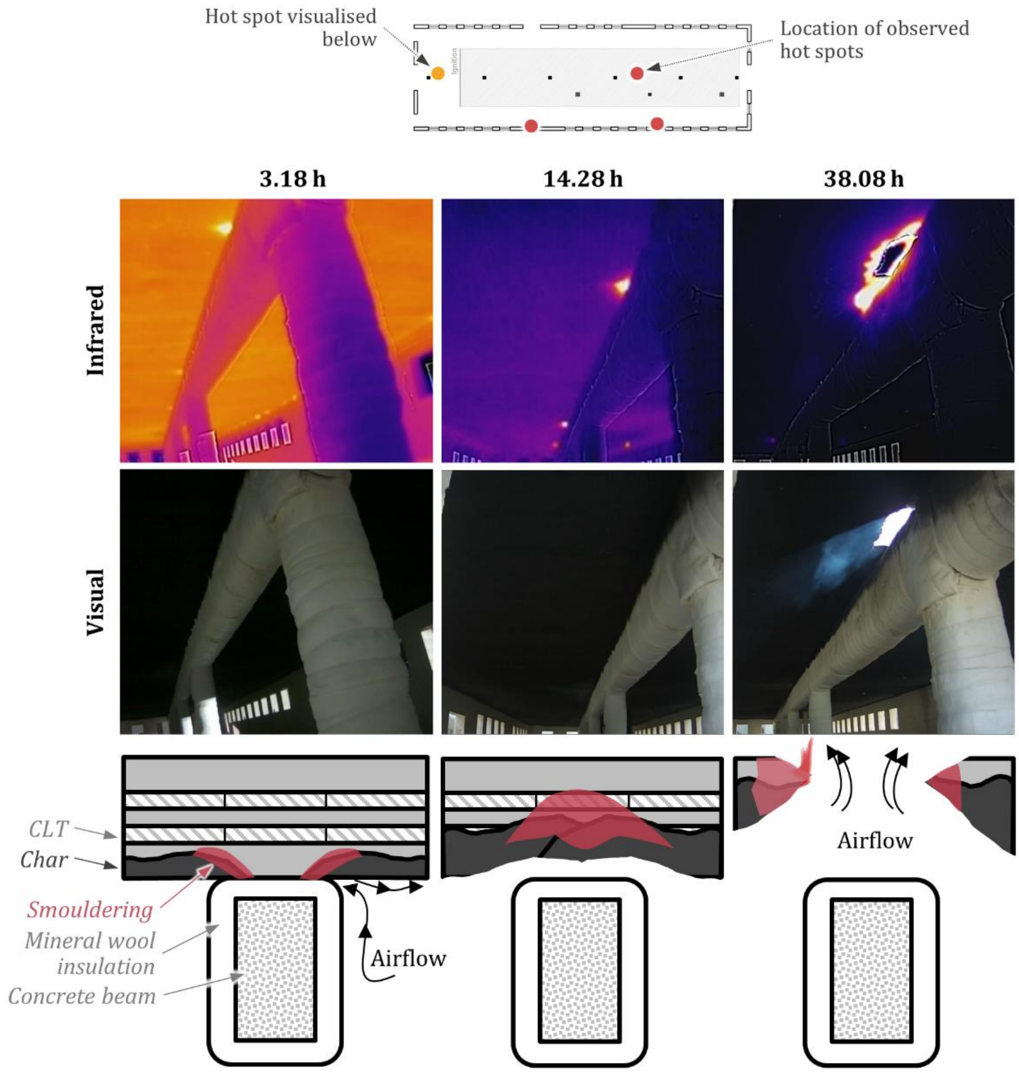

Figure 19. Position and development of smouldering hotspots in the CLT ceiling at three points in time. The diagram at the top indicates the locations of the smouldering hot spots. The top row shows Infrared (IR) images of the CLT ceiling, with the white regions indicating regions of high IR radiation. The middle row shows images of the ceiling in the visible spectrum. The bottom row contains diagrams illustrating the development of the large hotspot near the ignition location, and visible in both the IR and visual images.

The largest hole formed over a 40 h period, resulting in an approximately 250 mm wide × 1300 mm long hole through the CLT slab (Figure 19). On several occasions smouldering was observed to transition to flaming combustion at this hotspot. Following a 23 min period of rain, the smouldering was observed to be extinguished, suggesting water was effective at extinguishing the smouldering hotspot. Further analysis of these hotspots will be delivered in a future publication.

3.8 External flaming

Temperature and visual image data were captured outside the compartment to allow both qualitative and quantitative analyses of external flaming. Figure 7 and Figure 20 show images capturing the extent of external flaming through the growth phase and peak burning period of the experiment.

The first indication of external flaming was observed at the ignition-end of the compartment at 3 min 20 s. This time coincides with the period during which flames were seen extending horizontally across the exposed CLT surface, ahead of the wood crib ignition front. Figure 7 shows that the external flaming region progressed from the ignition-end to the far-end of the compartment between 3 min 40 s and 5 min 40 s after ignition.

The extensive external flaming through all openings of the compartment was observed 6 min (see Figure 20) after ignition in the order of 2.5 to 3 m in height. After this time, the location of the greatest external flame height moved along the compartment from the ignition end to the other end of the compartment. External flaming ceased from both the west and north door openings after 15 min (see Figure 20, camera views A and B*) while external flaming was still reaching heights of up to 1.5 to 2.5 m above the window and door openings at the far-end (East) of the compartment (away from the ignition location, camera views C* and D) as indicated by the height markers provided in Figure 20.

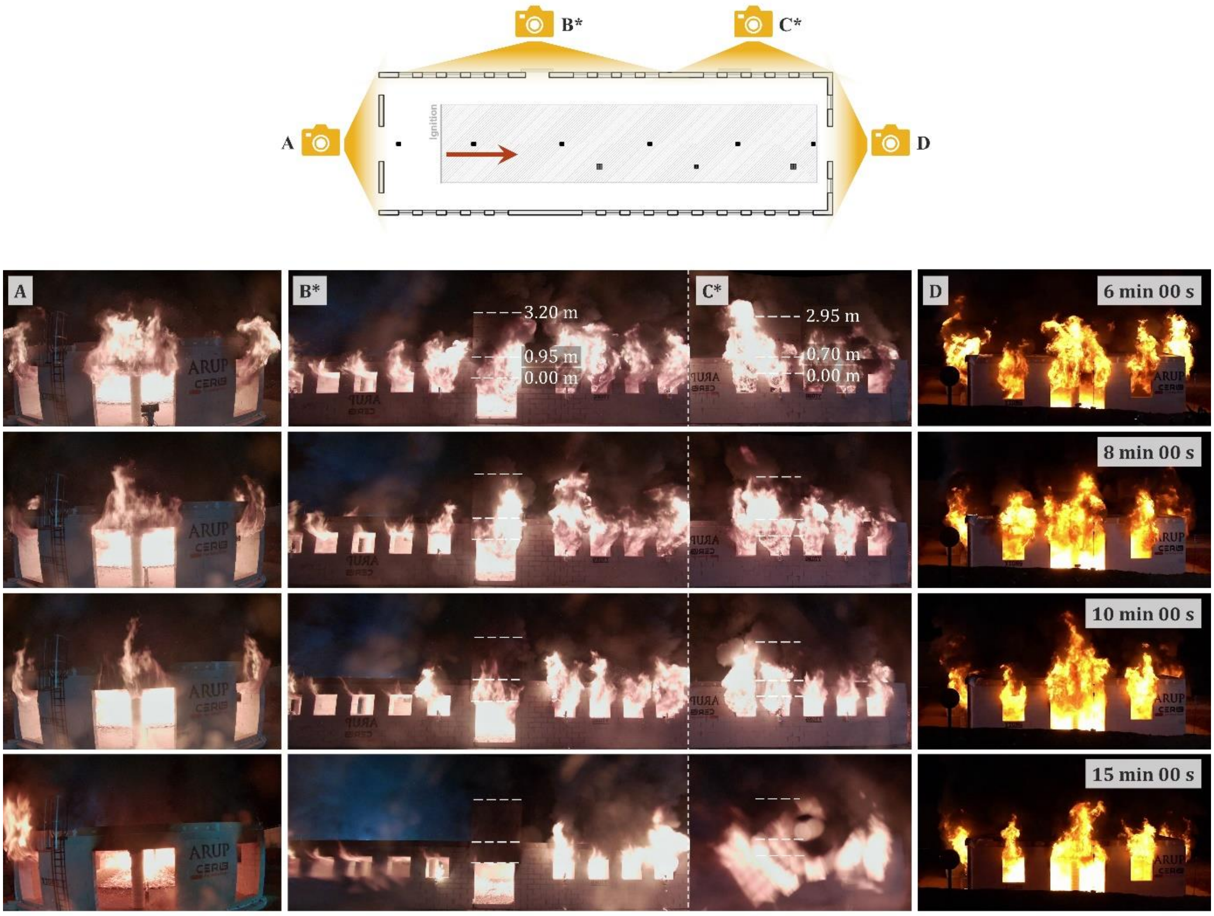

** Image is mirrored to show the fire travelling from left to right*

Figure 20. Selection of images captured during the experiment showing the size and progression of the external flaming observed during the peak burning period. Earlier timesteps are shown in Figure 7. The times annotated are the duration since ignition.

The gas phase temperatures recorded in the external flame/plume regions and the incident heat flux to the two façade panels are presented in Figure 21. The incident heat fluxes have been calculated from the temperatures recorded by the façade plate thermometers using Eq. (2). All data has been smoothed using the Savitzky-Golay filter [27] available within SciPy, using a time frame of 60 s and a 2nd order polynomial, to reduce noise.

Gas phase temperatures recorded at the external screen surface were generally lower than gas temperatures recorded at a 300 mm offset from the external screen surface. The screen thermocouples reached a maximum temperature of approximately 400°C for the door opening and 500°C for the window opening, whereas the 300 mm offset thermocouples reached over 800°C for the door opening and over 900°C for the window opening. This indicates that the external flame did not adhere to the external screen. This is expected to be due to high horizontal jet velocities of the gaseous volatiles leaving the compartment as opposed to wind, which was recorded as being negligible throughout the experiment (as detailed in Section 2.6).

The incident heat flux to both façade panels is presented in Figure 21. The initial peak heat flux to the façade above the door opening (~115 kW/m^2 at 5 min 40 s after ignition) is similar to the peak heat flux incident on the window opening screen (~110 kW/m^2 at 8 min after ignition). There is a delay of around 2 min 20 s in the window opening reaching maximum heat flux compared to the door opening, which is reflective of the opening positions relative to the ignition location. The initial peak heat flux above the door opening correlates with the initial peak gas phase temperatures above the door.

The external screen above the door opening experiences similar incident heat flux values at both 50 mm and 950 mm above the opening soffit, whereas the window opening façade screens experienced lower incident heat fluxes at 700 mm compared to 50 mm above the soffit, with a difference of around 20 kW/m^2 observed on average. This suggests that the external flame at the door opening had a greater volume at peak external temperature compared to the window opening's external flame, which is also seen in the gas temperatures.

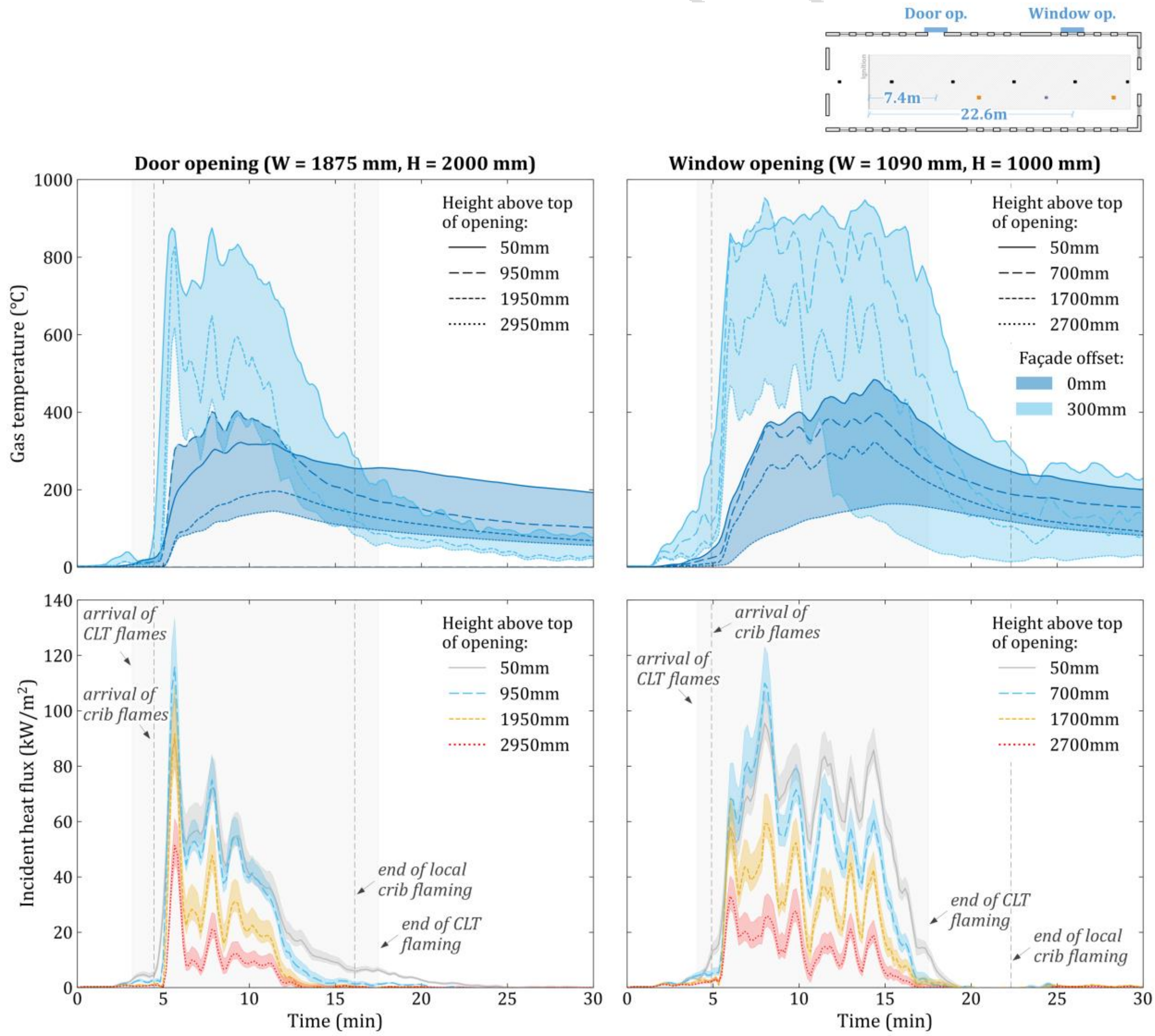

Figure 21. External flame / plume gas temperatures and incident heat fluxes to the façade measured at various heights above the opening soffit. The cloud in the incident heat flux plots

represents the maximum and minimum heat fluxes of all permutations of uncertainty in emissivity (0.7 to 0.9) and the heat transfer coefficient (5 to 25 W/m^{2}K [9]).

From observing images captured throughout the experiment (Figure 7 and Figure 20) and the temperature data presented in Figure 21, the duration of greatest external flaming was estimated as 5 min for the door opening (from 5 min 30 s to 10 min 30 s after ignition) and 9 min for the window opening (from 6 min to 15 min after ignition), to the nearest 30 s, representing a period with extensive external flaming equivalent to 22 % to 40 %, respectively, of the total flaming combustion duration of 22 min 30 s.

The crib trailing edge passed the door opening at approximately 16 min and then the window opening at 17 min 30 s after ignition. Once the crib fuel load was consumed, the external flaming decreased.

These observations indicate that the size of external flaming is dependent upon the opening dimensions (as suggested by existing external flame correlations [20]). Furthermore, the position of the opening relative to the ignition location also seems to have an influence in large-scale compartments, where travelling fires may be observed.

4 DISCUSSION

The experiment undertaken offers new knowledge about fire dynamics in large open-plan compartments with exposed timber ceilings. Understanding the effect of exposed timber on fire dynamics can impact all aspects of a fire strategy including means of escape, structural fire resistance and compartmentation, external fire spread and fire-fighting arrangements. Several fire research topics of interest for CLT compartments have also been identified below.

Faster fire spread

Rapid flame spread was observed across the ceiling following the ignition of the CLT. By comparison with similar experiments without CLT (*x-ONE* [11] and *x-TWO.1* [17]), the presence of CLT ceiling significantly increased the spread of the flame over the cribs on the ground. Based on the times reported for the flames from the crib to impinge on the ceiling and the arrival time of the leading edge of the fire to reach the end of the crib, the fire spread across the crib in *CodeRed #01* was 160 mm/s, while for *x-ONE* and *x-TWO.1* it was 73 and 35 mm/s, respectively. This increase in spread rate is most likely due to radiation heat transfer preheating the crib, resulting in a faster fire growth than in previous experiments with the same configuration in a non-combustible enclosure.

From these results it is clear that fire strategies for timber buildings must consider the fact that fires, in compartments without suppression, could spread significantly – 3 to 8 times in this case- faster than in equivalent non-combustible compartments due to the presence of the combustible timber at the ceiling.

Travelling fires with CLT ceiling

The fire travelled across the compartment length with clear leading and trailing edges. The spread rate of the leading edge was so much faster than the trailing edge that it resulted in a period of 6 min 24 s, or 28 % of the total flaming combustion period, in which most of the compartment was burning simultaneously. This fire behaviour is not like the traditional flashover [9] as it was not sudden and was non-uniform, but previous studies have refereed to similar phenomena as "localised flashover" [28].

Furthermore, while the peak gas phase temperatures were like those in non-combustible compartments (~1000°C), the temperature distribution showed large temperature variations throughout the compartment. Applying uniform flashover conditions to large compartments for some types of structures that are sensitive to non-uniform compartment temperatures such as steel frames may yield unconservative structural responses [29]. Further analysis should be undertaken for timber framed structures to investigate the impact of temperature non-uniformity. The presence of the CLT on the ceiling produced temperature profiles unlike the travelling fire methodologies in the literature [13] which have been developed for non-combustible ceilings. Temperatures near the ceiling were independent of distance along the compartment, while closer to the floor temperatures decreased sequentially with distance, due to the movement of the trailing edge. Further research and development is required to incorporate such dynamics into travelling fire methodologies for CLT compartments. Nevertheless, the travelling behaviour occurs so rapidly that further review is also needed to determine if design fires that are based on simpler flashover assumptions would yield sufficiently conservative results from a fire safety engineering perspective for structures that are not sensitive to non-uniform temperatures.

Longer fire duration, increased heat release rate and external flaming

The CLT ceiling can affect the fire duration. Compared to similar experiments without CLT (*x-ONE* [11], *x-TWO.1* [17]), *CodeRed #01* lasted approximately 2.5 min (11%) longer than *x-ONE* and 9.5 min (42%) longer than *x-TWO.1*, despite the fire in *CodeRed #01* growing more rapidly during its initial stage before touching the ceiling and therefore these time differences are not solely due to the presence of the ceiling.

The CLT ceiling also impacts the total heat release rate substantially, nearly doubling the peak HRR observed in the comparable non-combustible compartment from 69 and 58 MW in *x-ONE* and *x-TWO.1*, respectively, to 121 MW in *CodeRed #01*. This extra heat release rate impacts the amount of external flaming, which is also influenced by the ventilation conditions and compartment characteristics. Further research should aim to quantify the overall HRR burning outside the compartment and the HRR corresponding to individual openings (doors and windows) such that they can be utilised by engineers for the development of design fires and external flaming models.

Significant external flaming was observed in the order of 2.5 to 3 m in height for the majority of openings, compared to smaller, localised flaming experienced in a similar non-combustible building (based on observation by attendees and of video imagery noting that no measurements are reported for *x-ONE* [11] and *x-TWO.1* [17]). Extensive external flaming was observed from the door and window equipped with an external screen which endured for approximately 22 % to 40 %, respectively, of the total flaming combustion over a period of 22 min 30 s duration.

This poses a risk of vertical flame spread up an external wall, and also to adjacent property.

The impact of exposed CLT on external flaming requires further analysis and comparison to results from non-combustible structures will be presented in a future paper. Future research should consider how the experimental results compare to established external flaming analysis methods and how the presence of timber may be included in these models to account for the extensive external flaming observed. This would enable design solutions to be identified, addressing the hazard of vertical fire spread to other floors of the building and external fire spread to adjacent built assets. The applicability of existing large scale façade fire tests also needs to be reviewed.

The decay of the flames

The decay of the flames was steady and no secondary growth of the fire took place. This observation is in agreement with previous understanding from small compartments that a single exposed horizontal timber surface may not lead to re-ignition after burning of the fuel bed has finished. Contributing to this was the selection of the MUF adhesive based CLT ceiling which was observed to maintain the glue-line integrity, such that there was no extensive char fall off, ultimately preventing fresh timber being exposed. However, it should be mentioned that this experiment did result in comparatively shallow charring depth due to the short duration of the fire and performance of the CLT should be assessed in future research with longer fire durations.

The CLT flaming was observed to cease nearly simultaneously across the length of the compartment once the flames from the crib no longer impinged on the CLT. This is may be due to the importance of the heat transfer from the crib in maintaining CLT burning, which also enabled the rapid spread of flames over the ceiling. As expected, it was observed that where the ceiling is impinged upon by the flames from the crib, the CLT can sustain flaming. This behaviour has also been termed as "self-extinguishment" although the term does not consider the potential for ongoing smouldering combustion so unfortunately significantly underplays the hazards that need to be considered when using timber.

Smouldering fire and residual burning

After the flames of the fuel bed and the CLT ceased a number of hotspots kept smouldering for several days afterwards. This resulted in continued charring and the formation of one large hole through the full thickness of the CLT slab. These observations demonstrate that smouldering fire needs to be taken into consideration as a potential structural threat to timber buildings for three reasons. Firstly, the smouldering hotspots are difficult to detect until most of the compartment has cooled down, and afterwards only infrared imaging can provide a level of certainly as the smouldering is not discernible to the naked eye within blackened (charred / soot stained) surfaces. Secondly, if not dealt with through firefighting, smouldering can continue for hours and days, continuing to reduce the residual loadbearing capacity of the timber. Partial collapse by smouldering could be the initiation event for a total collapse, e.g. if affecting multiple loadbearing columns. Thirdly, smouldering hotspots can transition back to flaming fire hours after the main fire had stopped. This necessitates potentially long periods of monitoring and detection after the main fire has ceased, to identify and extinguish smouldering hot spots within the timber structure.

Future Research Needs

Future research should focus on comparing the fire dynamics observed with those in the non-combustible compartment as well as a detailed review of the smouldering, external flaming, CLT, and glulam performance and their impact for design purposes. Additional experiments are also planned to be undertaken at the same facility considering other parameters on fire dynamics such as (but not limited to) ventilation, fuel load, and encapsulation.

5 CONCLUSIONS

This paper presents novel experimental evidence from *CodeRed #01*, the first in a series of fire experiments carried out inside a purpose-built, open-plan to capture fire dynamics in large compartments with exposed timber. The experiment had an area of 352 m^2 and included a CLT ceiling and two glulam columns. The fire dynamics were captured via thermocouples, plate thermometers, as well as fixed and drone mounted cameras.

The main findings from the observations of *CodeRed #01* are summarised below:

- Rapid fire spread was observed across the CLT ceiling once the ceiling ignited. Fire spread via the ceiling, and reached the other end of the compartment more than 1 minute earlier than the fire spread across the wood crib on the floor. Compared to similar non-combustible enclosure experiments the fire spread was significantly faster. Any increase in speed of fire spread impacts occupant evacuation options, and fire-fighting response scenarios. Better understanding of the speed and duration of the fire enables robust design solutions to be developed.
- The CLT ceiling contributed significantly to the overall heat release rate of the fire contributing approximately the same energy as the fuel load of the wood crib. The increased heat release needs to be accounted for given its potential impact on structural fire resistance and the resulting more extensive external flaming.
- Flaming combustion of the CLT ceiling stopped almost simultaneously as the flaming of the fuel bed ceased to directly impact the ceiling. The MUF based CLT ceiling maintained glue-line integrity (i.e. there was no extensive char fall off) resulting in

predictable behaviour when exposed to fire as no new timber was exposed late in the fire at the ceiling;

- A significant portion of the pyrolysis gases burnt externally, evident in the substantial and prolonged external flaming observed above the openings. This impacts the speed and extent of vertical fire spread over the external wall within the same building, again relevant for evacuation options, and fire-fighting response scenarios. It is also important for the evaluation and control of external fire spread to adjacent built assets.
- The lower portion of glulam columns may experience increased charring due to the prolonged heat transfer from the surrounding embers remaining of the burnt wood crib; again relevant when designing structural fire resistance of vertical loadbearing timber elements, and also firefighting tactics.
- Without firefighting intervention smouldering continued throughout the monitoring period of 48 hours, and resulted in burn through the entire CLT slab depth in one location. This finding is relevant for fire-fighting tactics for timber buildings, and is an important consideration for the design of joints, junctions and connections.
- The decay of the fire was steady and no secondary flashover took place.

The impact of the findings from the observations of *CodeRed #01* on fire safety design and life safety of occupants and fire-fighters, fire-fighting tactics and property protection needs to be studied and tools and guidance need to be developed for practicing engineers and builders to safely construct with mass timber.

ACKNOWLEDGMENTS

This research has been fully funded by Arup and was undertaken in partnership with Imperial College London. The experiment was carried out at CERIB's Fire Test Laboratory site in France. All CERIB staff involved in the experiment are gratefully acknowledged as well as the two Imperial College London PhD students funded by EPSRC and Arup that travelled from the UK to France to work at the site despite the challenges and restrictions associated with the covid pandemic. The following Arup staff that helped in the analysis included in this work are acknowledged Clara Bermejo Bordons, Alexandra Dakin, Tess Van Der Veen and Daniel Thompson. We would also like to extend our heartfelt thanks to the steering group guiding the project, which includes Dr. Susan Lamont, Alistair Murray, Andrew Lawrence and Dr. Clare Perkins.

Statement of authorship

All persons who have meet authorship criteria in this manuscript are listed as authors. These authors certify that they have participated sufficiently in the work to take public responsibility for this manuscript's content, including the participation in the concept, design, analysis, writing, and revision of this manuscript. Those that do not meet this criteria are listed in the acknowledgements.

REFERENCES

1. Richter, F.Atreya, A.Kotsovinos, P.and Rein, G., (2019), "The effect of chemical composition on the charring of wood across scales," *Proceedings of the Combustion Institute*, Vol. 37, No. 3, pp. 4053–4061.

2. Hadden, R.M.Bartlett, A.I.Hidalgo, J.P.Santamaria, S.Wiesner, F.Bisby, L.A.Deeny, S.and Lane, B., (2017), "Effects of exposed cross laminated timber on compartment fire dynamics," *Fire Safety Journal*, Vol. 91, No. February, pp. 480–489.

3. Bartlett, A.I.Hadden, R.M.Hidalgo, J.P.Santamaria, S.Wiesner, F.Bisby, L.A.Deeny, S.and Lane, B., (2017), "Auto-extinction of engineered timber: Application to compartment fires with exposed timber surfaces," *Fire Safety Journal*, Vol. 91, No. March, pp. 407–413.

4. Emberley, R.Putynska, C.G.Bolanos, A.Lucherini, A.Solarte, A.Soriguer, D.Gonzalez, M.G.Humphreys, K.Hidalgo, J.P.Maluk, C.Law, A.and Torero, J.L., (2017), "Description of small and large-scale cross laminated timber fire tests," *Fire Safety Journal*, Vol. 91, No. March, pp. 327–335.

5. Su, J., Lafrance, P.-S., Hoehler, M.S., and Bundy, M.F., "Fire safety challenges of tall wood buildings – phase 2: task 2 & 3 – cross laminated timber compartment fire tests," 2018.

6. McNamee, R.Zehfuss, J.Bartlett, A.I.Heidari, M.Robert, F.and Bisby, L.A., (2020), "Enclosure fire dynamics with a cross-laminated timber ceiling," *Fire and Materials*, No. July.

7. Brandon, D., Sjöström, J., Hallberg, E., Temple, A., and Kahl, F., "Fire safe implementation of visible mass timber in tall buildings – compartment fire testing," 2020.

8. Zelinka, S.L., Hasburgh, L.E., Bourne, K.J., Tucholski, D.R., and Ouellette, J.P., "Compartment fire testing of a two-story mass timber building," 2018.

9. Drysdale, D., *An Introduction to Fire Dynamics*, 2nd ed. Chichester, UK: John Wiley & Sons, Ltd, 2011.

10. Rackauskaite, E.Kotsovinos, P.and Barber, D., (2021), "Letter to the Editor: Design Fires for Open-Plan Buildings with Exposed Mass-Timber Ceiling," *Fire Technology*, Vol. 57, No. 2, pp. 487–495.

11. Stern-Gottfried, J. and Rein, G., (2012), "Travelling fires for structural design–Part I: Literature review," *Fire Safety Journal*, Vol. 54, pp. 74–85.

12. Stern-Gottfried, J. and Rein, G., (2012), "Travelling fires for structural design-Part II: Design methodology," *Fire Safety Journal*, Vol. 54, pp. 96–112.

13. Torero, J.L.Majdalani, A.H.Cecilia, A.E.and Cowlard, A., (2014), "Revisiting the compartment fire," *Fire Safety Science*, Vol. 11, pp. 28–45.

14. Gupta, V.Hidalgo, J.P.Cowlard, A.Abecassis-Empis, C.Majdalani, A.H.Maluk, C.and Torero, J.L., (2021), "Ventilation effects on the thermal characteristics of fire spread modes in open-plan compartment fires," *Fire Safety Journal*, Vol. 120, No. April 2020, p. 103072.

15. Richter, F.Kotsovinos, P.Rackauskaite, E.and Rein, G., (2021), "Thermal response of timber Slabs exposed to travelling fires and traditional design fires," *Fire Technology*, Vol. 57, No. 1, pp. 393–414.

16. Rackauskaite, E.Bonner, M.Restuccia, F.Fernandez Anez, N.Christensen, E.Roenner, N.Wegrzynski, W.Turkowski, P.Tofilo, P.Heidari, M.Kotsovinos, P.Vermesi, I.Richter, F.Hu, Y.Jeanneret, C.Wadhwani, R.and Rein, G., (2021), "Fire experiment inside a very large and open-plan compartment: *x-ONE*," *Fire Technology*.

17. Heidari, M., "Travelling fires methodology and probabilistic design of structures," Imperial College London, 2021.

18. CEN, *EN 1991-1-2:2002 - Eurocode 1. Actions on structures. General actions. Actions on structures exposed to fire*. Brussels, 2002.

19. Pope, I.Hidalgo, J.P.and Torero, J.L., (2021), "A correction method for thermal disturbances induced by thermocouples in a low-conductivity charring material," *Fire Safety Journal*, Vol. 120, p. 103077.

20. Margaret, L. and O'Brien, T., *Fire and steel construction: Fire safety of bare external structural steel*. The Steel Construction Institute, 1981.

21. Bullen, M.L. and Thomas, P.H., (1979), "Compartment fires with non-cellulosic fuels," *Symposium (International) on Combustion*, Vol. 17, No. 1, pp. 1139–1148.

22. Abecassis-Empis, C., "Analysis of the compartment fire parameters influencing the heat flux incident on the structural façade," The University of Edinburgh, 2010.

23. Gorska, C.Hidalgo, J.P.and Torero, J.L., (2021), "Fire dynamics in mass timber compartments," *Fire Safety Journal*, Vol. 120, No. April 2020, p. 103098.

24. Ingason, H. and Wickström, U., (2007), "Measuring incident radiant heat flux using the plate thermometer," *Fire Safety Journal*, Vol. 42, No. 2, pp. 161–166.

25. Byström, A.Cheng, X.Wickström, U.and Veljkovic, M., (2013), "Measurement and calculation of adiabatic surface temperature in a full-scale compartment fire experiment," *Journal of Fire Sciences*, Vol. 31, No. 1, pp. 35–50.

26. Special Metals Corporation, "Inconel alloy 600, SMC-027," 2008. [Online]. Available: https://www.specialmetals.com/documents/technical-bulletins/inconel/inconel-alloy-600.pdf.

27. Savitzky, A. and Golay, M.J.E., (1964), "Smoothing and differentiation of data by simplified least squares procedures.," *Analytical Chemistry*, Vol. 36, No. 8, pp. 1627–1639.

28. Hidalgo, J.P.Goode, T.Gupta, V.Cowlard, A.Abecassis-Empis, C.Maclean, J.Bartlett,

A.I.Maluk, C.Montalvá, J.M.Osorio, A.F.and Torero, J.L., (2019), "The Malveira fire test: Full-scale demonstration of fire modes in open-plan compartments," *Fire Safety Journal*, Vol. 108, No. May, p. 102827.

29. Rackauskaite, E.Kotsovinos, P.Jeffers, A.and Rein, G., (2017), "Structural analysis of multi-storey steel frames exposed to travelling fires and traditional design fires," *Engineering Structures*, Vol. 150, pp. 271–287.